HHS Public Access

Author manuscript

Nanoscale. Author manuscript; available in PMC 2020 March 14.

Published in final edited form as:

Nanoscale. 2019 March 14; 11(11): 4634–4652. doi:10.1039/c8nr10059d.

Recent Development of Carbon Quantum Dots Regarding their Optical Properties, Photoluminescence Mechanism, and Core Structure

Keenan J. Mintz[a], **Yiqun Zhou**[a], and **Roger M. Leblanc**[a,*]

[a] Department of Chemistry, University of Miami, Coral Gables, Florida 33146 (USA).

Abstract

Carbon quantum dots (CDs) are a relatively new class of carbon nanomaterials which have been studied very much in the last fifteen years to improve their already favorable properties. The optical properties of CDs have drawn particular interest as they display the unusual trait of excitation-dependent emission, as well as high fluorescence quantum yields (QY), long photoluminescence (PL) decay lifetimes, and photostability. These qualities naturally lead researchers to apply CDs in the field of imaging (particularly bio-imaging) and sensing. Since the amount of publications regarding CDs has been growing nearly exponentially in the last ten years, many improvements have been made in the optical properties of CDs such as QY and PL lifetime. However, a great deal of confusion remains regarding the PL mechanism of CDs as well as their structural properties. Therefore, presented in this review is a summary and discussion of the QYs and PL lifetimes reported in recent years. The effect of method as well as precursor has been evaluated and discussed appropriately. The current theories regarding the PL mechanism of CDs are discussed, with special attention to the concept of surface state-controlled PL. With this knowledge, the improvement of preparation and applications of CDs related to their optical properties will be easily accomplished. Further improvements can be made to CDs through the understanding of their structural and optical properties.

Graphical Abstract

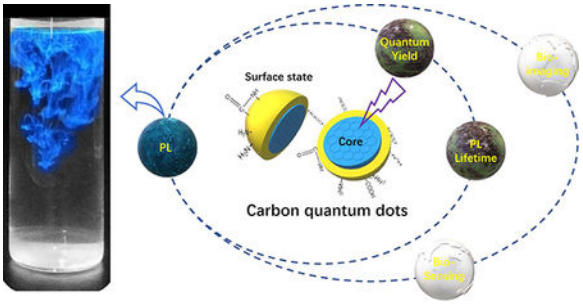

* Corresponding Author: rml@miami.edu.

1. Introduction

Carbon quantum dots (CDs) were discovered in 2004 when Xu et al. were attempting to prepare single walled carbon nanotubes. However, during characterization of carbon nanotubes they found a group of “fluorescent Nanoparticles”. [1] Since then, great strides have been made in the preparation of different types of CDs with much improved photoluminescence (PL) properties compared to when CDs were first studied, though the mechanism of PL is still not well understood.[2] However, the favorable optical properties of CDs, such as excitation-dependent PL, high fluorescence quantum yield (QY), and long PL lifetime, have prompted much attention toward the development of CDs for bio-imaging and sensing.[3–7] As seen in Scheme 1, the number of citations regarding QY and PL lifetime has grown exponentially over the last ten to fifteen years. This has led to a vast amount of literature for CDs, with many papers using different methods and precursors, which has added to the confusion that surrounds CDs PL mechanism, as many different explanations regarding the phenomena surrounding CDs are different. Comparison of these methods is needed to show the greatest improvements that have been made in the literature in recent years.

Since they were discovered, CDs have been viewed as a less toxic alternative to traditional quantum dots and very promising for the use in bio-imaging and sensing.[8, 9] CDs preparation is classified in two ways: top-down and bottom-up approaches. Top-down approaches utilize large carbon structures such as charcoal or carbon powder and cut them down to nanometer sized particles through methods such as laser ablation and chemical oxidation.[10, 11] Bottom-up approaches use small organic molecules or salts as precursors and under harsh conditions (e.g. high temperatures or microwave) the precursors will be carbonized to form CDs.[5, 12] When prepared, as previously mentioned, CDs are often characterized by their optical characteristics. A great deal of research has been made to improve the PL of CDs, particularly their QY. Several different factors can affect the optical properties of CDs upon production such as: method, precursor, passivation, and heteroatom doping. Common methods include laser ablation, microwave, and hydrothermal.[13] These methods generally provide different results, although no study has been done to compare them under similar conditions. The precursors presented in CDs literature are extensive, as virtually any carbon source could be used as a CDs precursor. Passivation of the as-prepared CDs is often achieved with polymers and/or small organic molecules containing heteroatoms (N, S, P, etc.).[14, 15] It has been shown that different types of precursors, surface passivation, or doping with elements such as nitrogen, sulfur, or boron can all result in higher QY and PL decay lifetime for CDs.[14, 16–19]

QY study is an important characterization for CDs because of their potential to be used as imaging agents in biological samples. In view of the great effort devoted on increasing the QY of CDs to improve their performance in this area,[20, 21] a systematic review of the progress made is needed. Different precursors, synthetic methods, and doping methods have been designed for this goal of increasing QY. In addition, the PL decay lifetime is an intrinsic property of CDs, which is usually on the low nanosecond scale. However, it can be tuned in different pH or temperature conditions.[22, 23] Also, the length of lifetime can be used to analyze the PL mechanism of CDs.[24] In addition, the increase of PL decay lifetime of

CDs is beneficial for the *in vivo* bioimaging as well as the expansion of a broad application of CDs. Therefore, it is of great significance of the theory study of the PL and structure of CDs.

There are two main points related to CDs which are not well understood. These are the mechanism by which they emit light and their core structure.[2, 25, 26] Many articles have been published endeavoring to elucidate these two points. Regarding the PL mechanism of CDs different theories have been published including: surface state[27, 28], quantum confinement[29, 30], and molecular state.[31, 32] Distinguishing between these phenomena is important to further the understanding of CDs as well as to aid in the rational design of CDs for specific applications.

Understanding the core structure is vital to understand the structural dynamics in CDs. Many applications rely on the surface of CDs (e.g. drug delivery) which is reasonably well-defined. However, to fully understand the interactions in CDs as well as the potential interactions of CDs in their application, the entire structure of CDs must be defined. Some have suggested graphitic cores[33], carbon nitride[34], or polymeric structures.[35] Determining the structural features of CDs is once again necessary for the rational design of CDs and for them to realize their full potential in a broad spectrum of applications.

There are currently several reviews for CDs in the literature. Zuo et al.[13] reviewed CDs bioanalytical applications. Wang et al.[36] presented CDs biological applications. Qu and coworkers[37] summarized heteroatom doping and bioimaging in CDs. Namdari et al.[38] focused on the biomedical applications of CDs. Zhou and coworkers[39] highlighted the quenching of CDs PL for sensing applications. Yan et al.[40] provided an overview of CDs' surface modification and functionalization. Huang and coworkers[41] discussed the sensing application of CDs. This review will present an overview of the current CDs preparation methods and precursors, and specifically how these two factors influence the QY and PL lifetime, and their applications in bio-imaging and sensing. For quick reference, a table is presented in supplementary information (table S1) which summarizes the properties of select CDs preparations. Then the current theories regarding the PL mechanism and core structure will be presented. The current literature expresses the unique ability of CDs due to their high QYs, long PL lifetimes and photostability, and compels further research to refine and better define this fast-growing field.

2. Developments in carbon dots' quantum yield based on precursor and preparation method

Quantum yield of PL is most commonly calculated through the use of a reference standard, although there are means to determine the absolute QY values. These require specialized and expensive instrumentation, while the use of a reference requires only traditional UV/vis and fluorescence spectrophotometers.[42, 43] QY (Φ) is defined according to equation 1, which states that it is the ratio of emitted photons to absorbed photons.

$$\Phi = \frac{\#\ of\ photons\ emitted}{\#\ of\ photons\ absorbed} \quad \text{Equation 1}$$

The most common way in which the value of QY for CDs is obtained, is according to equation 2:

$$\Phi_{CDs} = \Phi_{ref}\frac{A_{ref}a_{CDs}}{A_{CDs}a_{ref}}\left(\frac{n_{CDs}}{n_{ref}}\right)^2 \quad \text{Equation 2}$$

Where A refers to the absorbance of the sample, a is the area under the integrated PL curve, and n is the refractive index of the solvents used for the measurements. In this way researchers have been able to easily determine the QY of CDs. As will now be discussed, the QY of CDs is highly influenced by method and precursor.

2.1 Laser ablation preparations

In 2008, Sun. et al. [44] applied laser ablation to carbon Nanoarticles to obtain CDs. Then they treated the as-prepared CDs with nitric acid and doped them through the addition of $Zn(CH_3COO)_2$ with NaOH or Na_2S to obtain ZnO doped CDs and ZnS doped CDs, respectively. Both products showed similar absorption spectra, and the QY was calculated upon excitation at 440 nm for both, using quinine sulfate as a reference. The ZnS-CDs showed QY result at 50%, whereas the ZnO-CDs showed a slightly lower QY at 45%. The difference between the QY of the two CDs is negligible based on these results. Although laser ablation has been shown to generate photoluminescent CDs, there has not been many CDs obtained from laser ablation that have been applied in the field of bio-imaging. CDs obtained with this method are generally used in sensing applications.[24, 45]

2.2 Microwave-mediated preparations

Another common method of synthesizing CDs is using microwave to pyrolyze the precursors. In 2014,Qu et al. [46] prepared CDs by mixing urea and citric acid in two ratios, 0.2:1 (CNP1-carbon Nanoarticle) and 2:1 (CNP2), in water, and microwaving the mixture at 650 W for 5 min. The obtained solid was dissolved in water and ethanol and centrifuged to remove larger particles. CNP1 aqueous solution showed a QY of 15% with maximum emission at 440 nm emission (360 nm excitation), and CNP2 aqueous solution showed a QY of 18% (maximum emission at 540 nm with 420 nm excitation). When the QY was measured in an ethanol solution, the value for CNP1 was unchanged, but CNP2 showed a slightly blue-shifted emission at 526 nm (420 nm excitation) with a QY of 36%. The increased QY of CNP2 as well as the green emission show the possible effects dopants (in this case urea as nitrogen dopant) can have on CDs. Another microwave-assisted synthetic method that has been used was reported by Choi et al.[17] in 2016, and can give more information on nitrogen doping as well as doping with heteroatoms (boron and nitrogen). They synthesized 4 types of CDs. The first (BN-CDs) was made from mixing boric acid, citric acid, and 1,2-ethylenediamine (EDA) in water and microwaving at 700 W for 2 min.

The second (N-CDs) was obtained with the same synthetic method without the presence of boric acid. The third (B-CDs) and fourth (CDs) were prepared using citric acid with and without, respectively, boric acid by a hydrothermal approach at 180 °C for 6 hrs because they were not able to obtain the desired CDs from the microwave-mediated synthesis of just citric acid. The highest QY was shown by BN-CDs with 80.8 ± 5.1% and N-CDs showed 40.2 ± 1.8% with emission at 455 nm (excitation 350 nm). B-CDs and CDs showed a QY of 1.2 and 2.1% respectively.[17] Nitrogen doping is well known to increase the QY of CDs as shown here,[47, 48] but the positive effect of adding an additional dopant of boron is shown as well as the QY jumps to over 80%. The comparison between CDs and B-CDs may not be reliable as QY for both are not apparently different (1–2%), however the increase in QY due to heteroatom doping can be still clearly seen in the microwave-mediated preparations.

In the same year, Yu et al. [49] were also able to synthesize highly photoluminescent CDs using a microwave-assisted synthetic approach. They mixed citric acid, PEG 400, and N-(2-hydroxyethyl) ethylenediamine in water, sonicated for 2 min, and heated in a microwave oven for 20 min at 800 W. The obtained solid was purified by dialysis and underwent optical characterization. Their obtained product showed an excitation wavelength-dependent emission with a QY of 79.63% at 447 nm (351 nm excitation). The ability of nitrogen to enhance the QY of CDs is again clearly shown here. The addition of the polymer, PEG 400, facilitated the formation of a hydrogel film of CDs, which showed an ability to detect Hg^{2+} ions based on the quenching effect of PL of CDs. Also, they were able to show a low detection limit of 0.089 μmol/L.

In 2017, Kudr et al.[50] synthesized CDs by using a microwave oven and employed them to detect DNA damage in PC-3 cells. They dissolved citric acid and diethylenetriamine (DETA) in water and placed in the microwave oven for 3 min at 800 W. They measured the QY to be 4% with maximum emission at 480 nm (360 nm excitation). They attributed this low QY to the extended dialysis time they used to purify the CDs. They also reported the fluorescence decay lifetime to be 12.8 ns as it was significantly long for DNA damage detection. When the CDs were mixed with ethidium bromide and DNA, CDs transferred energy to ethidium bromide through a FRET process and the fluorescence observed was dependent on the DNA damage.

Another method assisted by microwave that will be discussed is from Roshni and Divya[51] They used sesame seeds as precursors of CDs and used a microwave oven at 800 W for 15 min. The QY reported was 8.02% with 440 nm maximum emission (365 nm excitation). They also conducted photostability tests by constantly irradiating the sample with UV light for 6 hrs. After 6 hrs, their CDs sample showed only a 5% decrease in fluorescence intensity.

2.3 Hydrothermal or solvothermal preparations

Another common synthetic method, of which some examples have already been discussed, is the hydrothermal or solvothermal approach. This approach will be discussed to see the effect of precursors on the QY of CDs. With this method, the most common precursor used as a carbon source is citric acid.

In 2017, Li et al.[52] used citric acid in conjunction with poly(ethylenimine) (PEI) to synthesize CDs. They heated the precursors up to 110 °C for 2 hrs in a tightly-sealed autoclave. This yielded a product with a pH dependent (optimum pH=4) QY of 48.3 ± 5.3% with a maximum emission of 459 nm (excitation of 360 nm). In 2017, Zhang et al. [47] and Lin et al.[48] published two articles in which citric acid and N-(b-aminoethyl)-g-aminopropyl methyldimethoxy silane (AEAPMS) were utilized as precursors for the preparation of CDs with a thermal method. The precursors were heated up to 220 °C in the presence of ethanol for 3 and 5 min, respectively. These products showed red-shifted emissions around 600 nm (580 and 610 nm, respectively) with a QY of 37% for 3 min and 19% for 5 min. Both products show an unusually long wavelength of PL for CDs formed from citric acid.[53, 54] The PL wavelength is red-shifted for the longer reaction time (5 min), but the QY is decreased by almost half. Both also show relatively long PL lifetimes of 12.55 ns (3 min) and 12.29 ns (5 min). Citric acid has been used with L-cysteine in a hydrothermal method to prepare CDs. This yielded an unusually short emission wavelength (418 nm), but with a high QY of 64%.[55] Citric acid has also been used as a CD precursor with a eutectic mixture of salts ($NaNO_3$/KNO_3/$NaNO_2$).[56] This method yielded a QY of 20.8% which is a lower value than those which have been reported for many other citric acid-based CDs. This could indicate the benefit of organic, nitrogen-containing compounds as heteroatom dopants and surface passivating agents. Chandra et al.[53] performed a study which follows the same trend. They used diammonium citrate as a CDs precursor and obtained CDs with a QY of 11.21%. [57] This is further emphasized in a study performed by Yang et al. in which aqueous ammonium citrate was used as the sole CD precursor.[58] This yielded a QY of 13.5% which is again lower than other citric acid/citrate based CDs which use organic nitrogen dopants.

In 2015, Wang et al. prepared three CDs from the reaction of urea with glycolic acid, malic acid, and citric acid (one, two, and three carboxylic groups, respectively).[59] They saw good correlation between the number of carboxylic groups with optical properties. The emission wavelength, PL lifetime, and QY (12.9, 32.4, and 54.9%, respectively) all increased with the number of carboxylic groups. This is attributed to the strengthened ability of citric acid to conjugate with the amine groups on urea, which decreases with malic acid and then with glycolic acid. These CDs were also shown to be good bio-imaging agents in cancer cell line MG-63.

The highest QY reported for CDs to date was in 2015 from Zheng et al. [22] They prepared CDs using citric acid and tris-(hydroxymethyl)aminomethane (tris) with a thermal method. This yielded CDs with emission at a short wavelength (417 nm) and an ultra-high QY of 93.3%. They attributed this high value to the nitrogen doping with tris which promotes radiative recombination for relaxation.

A common precursor that is often paired with citric acid to synthesize CDs is EDA. In 2017, Zhou et al.[60, 61]prepared CDs using citric acid and EDA in a 1:14 molar ratio with a solvothermal method of varying temperatures. The optimum conditions reported were heating the precursors to 160 °C for 1 hr. The obtained product was a very viscous gel-like CDs which provided a QY of 33.7% with a maximum emission of 450 nm (excitation of 350 nm). After a series purification by acetone wash and separation by thin layer chromatography, four CDs fractions were obtained. Among the four fractions, there was one

fraction exhibited excitation-independent PL with a QY of 55%, which was almost double the QY of the initial gel-like CDs.[62] Wen et al.[63] also used citric acid and EDA as CDs precursors. Using a furnace, they heated the mixture to 200 °C for 4 hrs and purified the raw product with size exclusion chromatography (SEC). Their two obtained fractions displayed wavelengths of emission of 460 and 530 nm, with QYs of 40.69% and 69.30%, respectively. In 2017, Parvin and Mandal[64] used citric acid and EDA as precursors, but also added H_3PO_4 to study the effect of adding another heteroatom, namely phosphorous. They heated their mixture to 250 °C for 2 hrs and filtered the product to remove the precipitate from the product. Their product showed typical excitation wavelength-dependent PL and they recorded the QY for two different excitation wavelengths, 360 and 440 nm. The QY was 30 and 78%, respectively. They demonstrated the utility of the obtained CDs by testing their imaging capabilities *in vitro* (in cell line RAW 264.7) and *in vivo* (in nude mice). There have been several studies which attribute the high QY from citric acid-based CDs to organic fluorophores which are generated during CDs preparation and incorporated into the CDs.[54, 55, 65] However, the vast majority of reports of this phenomenon are only concerning citric acid derived-CDs, and this effect cannot be extrapolated to discuss all CDs.

EDA has also been used as a precursor in preparations that do not involve citric acid. In 2015, CDs were prepared from alanine and EDA through a hydrothermal method. The resulting CDs possessed a QY of 46.2% with maximum emission of 390 nm.[66] These showed potential application in cellular imaging and in sensing of NADH. In 2017, Tao et al.[67] used polyacrylic acid and EDA to prepare CDs. These CDs displayed emission at 450 nm and a QY of 44.2%. Yang et al.[68] used ethanediamine, an isomer of EDA, with C_3N_4 (carbon nitride) to prepare CDs, which showed a QY of 21% and maximum emission wavelength of 470 nm. There PL intensity also exhibited temperature dependent- behavior. This property enabled the CDs to be used as both *in vitro* and *in vivo* temperature probes in HeLa cells and mice, respectively. Tryptophan has been used with EDA to prepare CDs with QY of 48.4%.[69] This value was significantly higher than the QY for the same reaction performed with urea replacing EDA (21.5%). This displays the high value of EDA as nitrogen dopant.

The importance of heteroatom doping to the QY of CDs cannot be understated and has been demonstrated by Xu et al.[70, 71] In 2017, they prepared nitrogen and phosphorous co-doped CDs through the use of sodium citrate and diammonium phosphate as precursors. These CDs displayed a QY value of 53.8% with excitation-dependent emission and good pH stability. Interestingly, when the ratio of sodium citrate to diammonium phosphate was decreased below 19:1, the level of heteroatoms decreased as well as the QY. The proposed explanation for this suggests that an excess of heteroatoms could block the surface defects reducing the efficiency of PL.

Metal atom doping is a strategy which is not commonly used but has been shown to increase CDs' QY substantially. Xu et al.[72] prepared CDs from sodium citrate, citric acid, and manganese carbonate which exhibited a QY of 54%. In this case citric acid was used in addition to sodium citrate to enhance the solubility of manganese carbonate. They also showed pH played an important role in the reaction, by showing the decrease of QY when larger amounts of citric acid were present in the reaction mixture. The metal carbonate bond

in the CDs was believed to be the important factor for enhancing the QY of the CDs. This group was shown to be more effective for this cause than the metal-carbon or metal-oxide bond. This has been the highest QY to date for metal-doped CDs.

As was previously discussed, nitrogen doping has often been used to improve CDs' QY. Unsurprisingly, nitrogen containing polymers have often been studied as CDs precursors. In 2013, branched polyethyleneimine (bPEI) and ammonium persulfate were used with a hydrothermal method to prepare CDs.[73] This yielded CDs with the maximum emission at 460 nm and a QY of 54.3% (350 nm excitation). These CDs were promising in cell imaging and gene delivery. In 2015, Yang et al.[74] prepared CDs using β-cyclodextrin, PEI, and phosphoric acid. This yielded a type of CDs with a QY of 30% with the maximum emission at 510 nm. These CDs demonstrated excellent capabilities as imaging agents and theragnostic carriers in association with hyaluronic acid, which is supported by the fluorescence bioimaging in Figure 1. Folic acid and PEI were applied with a 180 °C hydrothermal method to prepare CDs in 2017. It yielded CDs with 450 nm emission and a QY of 42%.[75] These also showed excellent capability in cellular imaging as well as the unusual CDs' trait of being positively charged, which provided applications for the CDs in delivery through the electrostatic association with DNA. These few examples above are representatives of CDs formed from PEI, which typically have blue emission and high QY.

Biological molecules and natural products have been used to prepare CDs as well. Yang et al. prepared CDs from glucose and monopotassium phosphate. The reaction yielded a low QY of 2.4% with 435 nm emission.[76] In 2014, L-tartaric acid, lauryl chloride, and D-glucose were used to prepare CDs which emitted in the highest intensity at 460 nm with a QY of 16.5%.[77] Because these CDs possessed an amphiphilic nature, they were able to be used to image cell membrane as seen in Figure 2. In 2017, aminosalicylic acid was used with ethanol as a precursor for CDs. The resulting CDs showed a maximum emission wavelength of 516 nm with a QYof 16.4%. These CDs were used as an *in vitro* sensor for Fe^{3+} in H1299 cells.[78] Xu et al.[79] produced CDs from casein, a common protein found in milk. These CDs possessed a QY of 31.8% at 446 nm emission, and their capabilities were shown in cellular imaging and also for detection of Hg^{2+} in HeLa cells. Aspartic acid was also used by Yang et al. to prepare CDs in 2017. They showed the maximum emission wavelength of 402 nm with a QY of 41.3%.[80] Abu-Ghosh et al. [81] prepared CDs from bovine serum albumin (BSA). These CDs yielded the maximum emission at 460 nm with a QY of 44%. The authors demonstrated the CDs utility in promoting algal growth through converting UV light from the solar spectrum to visible blue light.

2.4 Foodstuff precursors in preparations

As was previously discussed, sesame seeds have been used to prepare CDs. Many other foodstuffs have also been used as CDs precursors. The QY of around 8% in Roshni et al.'s study[51] is similar to other QY reported for processes involving foodstuffs, such as the study reported by Zhou et al. where watermelon peel was used as a precursor. The peel was carbonized at 220 °C for 2 hrs, purified by dialysis to acquire CDs. They obtained a QY of 7.1% with maximum emission at 490 nm (excitation 340 nm).[82] In 2013, De and Karak[83] used banana juice as a CDs precursor, mixing it with ethanol and heating to 150 °C in an

oven for 4 hrs. Their obtained QY was 8.95% with maximum emission at 460 nm (excitation 360 nm). In 2014, Wang and Zhou[84] synthesized CDs from milk with a hydrothermal method at 180 °C for 2 hrs. Their obtained QY was 12% with maximum emission of 454 nm (excitation 360 nm). To examine the potential of their CDs in the cellular imaging they also did photostability experiments and found that after continuous excitation at 365 nm for 3 h the fluorescence intensity did not decrease. In addition, they reported that the CDs retained 90% fluorescence intensity after storage for 6 months at 4 °C. Since the CDs were stable, they labeled U87 cells and imaged the cells with confocal microscopy, which is shown in Figure 3.

Interestingly, Mandani et al.[85] discovered that CDs are naturally present in honey. These CDs possessed blue emission (456 nm) with a QY of 1.6%. Due to the low QY, these CDs are limited in application. However, this represented the first time CDs have been shown to naturally occur.

One more foodstuff precursor example was discussed in 2016 when Liu et al.[86] synthesized CDs from carrot juice using a hydrothermal method at 160 °C for 6 hrs. Their CDs showed a QY of 5.16% with emission at 442 nm (excitation 360 nm). They then did cell viability and imaging tests with a HaCAT cell line. The viability test showed that over 85% of the cells remained viable with a high concentration of 700 μg/mL CDs. The imaging results that they obtained using confocal microscope are shown in Figure 4.

As shown in the examples mentioned above, the “top-down” synthetic approach of CDs using foodstuff precursors did not result in a high QY. However, the CDs obtained through these methods have been widely applied in sensing and imaging.

As has been discussed, there is a vast amount of preparation methods for CDs in the literature today. Hydrothermal and microwave methods often produce higher QY values than other procedures. Concerning precursors, heteroatom doping with elements such as boron, nitrogen, and phosphorous is an important strategy to increase the QY of CDs. The amount of methods and QY values can lead to some discrepancies, but the potential of CDs as optical probes through high QYs has been established repeatedly. Now the focus will turn to another important optical property.[87]

3. Developments in carbon dots’ photoluminescence lifetime

PL decay lifetime of CDs indicates the time CDs spend in the excited state before returning to the ground state with the emission of photons.[88] The PL lifetime can only be measured using time resolved spectrophotometers, and is commonly measured using femtosecond laser pulses.[89] Considering the stable and constant PL required, the length of PL decay lifetime is also an important indicator to measure if the obtained CDs have great potential regarding application in the solar cells,[90] bioimaging and sensing fields especially as intracellular probes for time-gated cellular detection.[91] Sensing is an especially important application related to PL lifetime as the analyte usually shortens the lifetime for CDs.[92] Besides, as was measured and reported by previous literatures, CDs possess a longer PL decay lifetime than most common fluorophores such as fluorescein, Rhodamine B, and

Alexa Fluor 488 and 647[93], which confirms CDs can serve as a biocompatible alternative to the common toxic fluorophores in *in vivo* tests. However, as mentioned before, the QY of CDs varies depending on different synthetic approaches and post-treatment[48, 94, 95], the PL decay lifetime is also different based on different fabrication methods.[68, 96] Therefore, in order to widely apply CDs into bioimaging and sensing experiments, besides the QY, the PL decay lifetime also needs to be prolonged. Here, we summarized the PL decay lifetime of CDs in recent years with the aim of comparing different syntheses and finding the best reaction conditions.

3.1 Top-down approaches for carbon dots' preparations

In 2011, Zhou et al.[82] obtained photoluminescent CDs by low-temperature carbonization (200 °C) of watermelon peel. As a typical representative of a "top-down" method, this preparation process is more facile and environmentally friendly than the other "top-down" methods considering the ease of the reaction conditions, including the low temperature and short production time as well as the availability of the precursor.[10, 97] Figure 5a showed the UV/vis absorption and PL emission spectra, which revealed the CDs, similar to most CDs, were excitation wavelength dependent[98–100] and the PL decay lifetime was measured with an acceptable value of 5.72±0.05 ns. In terms of application, the strong blue PL and sufficient PL decay lifetime ensured the CDs could work as a good imaging probe when they were incubated with Hela cells (Figure 5b).

Lamp or candle soot[101, 102] after burning is always an optimal candidate as the precursor of CDs. Liu[93] and Kumar[103] have successively prepared CDs with lamp or candle soot as the initial carbon source. And in order to improve the PL emission ability, Liu et al.[20] dispersed the candle soot into 25 M NaOH aqueous solution to fabricate fluorescent hydroxyls-coated CDs with a PL decay lifetime of 9.5 ns, which indicates the radiative recombination nature of excitons. The advantage of hydroxyl-coated CDs over the regular carboxyl-coated CDs was the surface hydroxyls had strong electron donation ability which would be beneficial for the PL emission while the surface carboxyl has a strong electron withdrawing ability that would reduce the PL intensity and the different surface states of CDs were illustrated in Figure 6a. In addition, due to the enriched hydroxyl surface, the obtained CDs was studied in the detection of metals and metal ions such as Hg^{2+}, Cr^{3+}, Al^{3+}, and Fe^{3+} would easily quench the PL of CDs which provided great opportunity for measuring Cr^{3+}, Al^{3+}, and Fe^{3+} in human fluids (Figure 6b). In Kumar and Bohidar's research paper[103], they studied the solvent dependent spectroscopy of a non-functionalized CDs made of lamp soot. The PL decay lifetime tests revealed the average lifetime didn't change in the aromatic solvents which was 4–5 ns, decreased with the polarity of hydrogen bonded solvents such as methanol and ethanol, and increase with the polarity of aprotic solvents such as acetonitrile.

In 2015, Nguyen et al.[24] performed femtosecond laser ablation of graphite powder within a polyethylene glycol (PEG_{200N}) solution to prepare CDs. As the PL mechanism of typical CDs is always under debate, researchers proposed two different pathways of electron-hole (exciton) radiative recombination to study the carrier (electron or hole) dynamics in CDs and each pathway had a relaxation time scale. For example, the relaxation of carriers from the carbogenic core to the surface of CDs Nanoarticles owned a relatively longer PL decay

lifetime (>14 ns) while the direct radiative recombination of the surface of CDs was much faster with a short decay lifetime of 1.3 ns. Also, they found when the excitation wavelength was short, the short decay lifetime was dominant which was explained by the relaxation of carriers from carbogenic core to the surface of CDs. Meanwhile, the long PL decay lifetime was measured when the excitation wavelength used was longer, which could be mainly due to the direct relaxation of carriers on the surface of CDs. The mechanism also worked to account for why some CDs are excitation wavelength dependent at longer wavelengths while independent at shorter wavelengths.

3.2 Bottom-up approach for carbon dots' preparations

In addition to the "top-down" approaches to synthesize CDs mentioned above, the "bottom-up" approaches are the other and more prevalent branch of the preparation strategy to create CDs. Regarding the initial materials, "bottom-up" approaches usually take use of small organic molecules such as citric acid,[104, 105] as previously discussed, as a monomer-like unit modified by amine compounds to fabricate polymeric CDs. Even though there seem more options, compared in terms of PL decay lifetime of CDs obtained from "top-down" approach, "bottom-up" approach doesn't show any apparent improvement.

With citric acid as the initial material, Yang et al.[58] in 2013 reported a nitrogen-doped carbon-rich CDs synthesized from ammonium citrate via a hydrothermal treatment. Interestingly, the CDs were excitation wavelength independent when they were excited from 245 to 395 nm and the emission wavelength was 437 nm measured from the PL spectrum (Figure 7a). The PL decay profile of the CDs shown in Figure 7b exhibited a single exponential decay kinetic of the CDs excited at 337 nm with a PL decay lifetime of 10.6 ns, which showed a relatively long radiative recombination of the excitons with PL emission.

As an excellent carbon source to prepare CDs, citric acid was again employed by Li et al.[106] in 2014 to synthesize highly photoluminescent CDs. The same preparation was performed at four different temperatures (130, 160, 200 and 240 °C) and the PL properties such as QY and PL decay lifetime varied depending on the amino-passivation degree of the surface of CDs which was determined by the reaction temperature (Figure 8a). In comparison, the CDs obtained at 160 °C owned the highest QY of 44.7% and the longest PL decay lifetime of 7.13 ns which was due to the highest amino-passivation on the surface. Another interesting difference between the CDs made at different temperatures was observed in the PL emission spectra. In the spectra, we can observe the CDs made at 160 °C are excitation wavelength independent while the CDs synthesized at 240 °C are excitation wavelength dependent (Figure 8b). The excitation wavelength independent behavior of CDs made at 160 °C relied on the single surface state, while as for CDs made at 240 °C, when excitation energy was higher than the energy gap, emission was no longer mainly related to the energy gap transition and it was controlled by the surface state transition. Also, the metal ion test showed the best quenching effect of Fe^{3+} and Be^{2+} on the CDs, which showed the selectivity and sensitivity of the CDs to Fe^{3+} and Be^{2+}, and the detection limit of toxic Be^{2+} was as low as 23.3 μM (Figure 8c).

In 2015, Liu et al.[97] prepared nitrogen doped CDs (N-CDs) by using citric acid and ammonium hydroxide through a hydrothermal route. Even though the PL decay lifetime and

QY have not been remarkably improved which were 40.5% and 9.03 ns, respectively, the selective detection of Hg^{2+} in real water with a detection limit of 0.087 μM was still of great significance due to the severe environmental and health problems caused by Hg^{2+}.[107]

In order to improve the PL behaviors of CDs, a great deal of research involving enormous efforts including the selection of the reaction precursors and optimization of the synthetic approach have been continually sought[108]. Zheng et al.[22] reported a novel pH-sensitive N-CDs with the highest QY (93.3%, as previously discussed) and longest PL decay lifetime (19.5 ns) among all the CDs reported so far. The whole synthesis took citric acid and tris-(hydroxymethyl)aminomethane (Tris) as precursors under 160 °C with the assistance of microwave digestion treatment for 10 min. The CDs in different pH environment exhibited different PL behaviors and based on different pH environments, the surface of the CDs was rich in H or OH, namely CDs-H and CDs-OH. The emission of CDs-H was found to be excitation wavelength dependent while that of CDs-OH was free of excitation wavelength dependence. Also, the PL decay lifetime was dependent on the emission wavelength for CDs-H while insensitive to emission wavelength for CDs-OH. The difference resulted from the uniform surface state of CDs-OH due to the deprotonation of carboxylic groups on the surface.

Compared between *in vivo* and *in vitro* experiment, CDs are more commonly tested as a potential probe for *in vitro* imaging and sensing. However, in 2016, Kalytchuk et al.[23] prepared CDs with an average size of 4.5 nm in diameter with citric acid as a carbon source and L-cysteine as the nitrogen and sulfur dopant of the CDs via a hydrothermal route. The CDs exhibited temperature-dependent PL lifetimes decay (Figure 9a) and their PL decay lifetime monotonically decreased from 11.0 to 5.3 ns as temperature increased from 2 to 80 °C. In addition, their PL lifetime was free of the wide variation of pH, concentration of CDs, and solution ionic strengths. Also, as the cell uptake and cytotoxicity experiment of CDs showed, the CDs have low toxicity and excellent biocompatibility, which laid the foundation of the CDs as an intracellular thermal sensor. As a result, the temperature, determined using the calibration curve based on the PL decay lifetime, extracted from PL transients recorded every 15 min for 24 h of the HeLa cells cultured in CDs aqueous solution agreed with that measured with a reference thermometer, and the absolute average accuracy of temperature detection was 0.27 °C (Figure 9b–e). Therefore, due to the low toxicity and sole temperature-dependent PL lifetime behavior, the CDs are a great Nanorobe of the intracellular temperature.

3.3 Development of Phosphorescence in carbon dots

Recently the exciting development of ultralong-lifetime, room-temperature phosphorescence has been observed in CDs. Lin and coworkers[109, 110] used phosphoric acid with either ethanolamine or EDA to generate CDs which displayed phosphorescence to the naked eye for up to 10 s. They showed the lifetime to be 1.46 and 1.39 s, respectively for the CDs made with ethanolamine and EDA. These CDs were used for security feature printing. As would be expected, the phosphorescence was quenched in solution and was only observed in the solid state. This phosphorescence was attributed to the doping of phosphorous into the CDs structure which produced the long lifetime emission.

Phosphorescence in CDs has also been achieved without doping phosphorous. Long et al.[111] used a solvothermal method with glucose and triethylamine trihydrofluoride to prepare CDs which exhibited phosphorescence with a lifetime of 1045 ms XPS data showed 14% nitrogen and 7% fluorine. They believed the phosphorescence was due to the low energy difference between the singlet and triplet states for the C-N/C=N bonds. Additionally, the semi-ionic nature of the C-F bond stabilized the triplet state and reduced quenching by oxygen. Similarly, Gao et al.[112] used glucose and aspartic acid to generate CDs with a phosphorous lifetime of 747 ms. Here they claim the poly-aspartic acid chains on the surface of the CDs creates a barrier to air and moisture under ambient conditions which disallows the quenching of emission in the solid state. Both previous examples allow phosphorescence through doping with heteroatoms which are not phosphorous. Other studies have shown that hydrogen bonding is an important factor in the phosphorescence of CDs.

In 2018, Li et al.[113] used citric acid and urea to generate CDs which were then passivated with cyanuric acid. These CDs surprisingly exhibited phosphorescence in an aqueous suspension with a lifetime of 687 ms. This lifetime was much higher than the lifetime for the dry powder which was 253 ms. This was attributed to the increased rigidity of the system introduced by the hydrogen bonding of water and cyanuric acid with the C=O bond of CDs. Hydrogen bonding also played an important role in a study by Yue and coworkers.[114] CDs prepared from citric acid and folic acid displayed a phosphorescence lifetime of 705 ms in pH 11.5. This basic pH displayed a longer lifetime than did neutral or acidic aqueous solutions. The basic pH enhanced the phosphorescence through deprotonating the carboxylic groups and increasing the conjugation of the electronic system. This in addition to the intraparticle hydrogen bonding greatly increased the lifetime and QY of phosphorescence.

4. Developments in understanding of carbon dots' photoluminescence mechanism

4.1 Current theories for PL mechanism of carbon dots

Soon after the discovery of CDs in 2004, researchers began to speculate regarding the nature of CDs' PL and why they possessed excitation-dependent emission.[87] Three main theories emerged, namely: quantum confinement, molecular state, and surface state.[30] The theory of quantum confinement in CDs was a natural inquiry to pursue, as metal-based quantum dots are well known to possess emission based on this phenomenon.[115] While there are several papers published using this explanation to explain the PL mechanism of CDs, it is not the most common as many CDs systems simply do not have the data to support this theory. Another common theory suggests the synthesis of different molecular fragments which are attached to the surface of CDs in the preparation process. This explanation is referred to as a "molecular state". There are many papers with strong evidence to support this theory, but the scope of this explanation is limited to certain CDs preparations. Several CDs preparations using citric acid have used this explanation for the PL mechanism.[116, 117] Additionally, there has been some studies, which used a fluorescent precursor in the preparation method, to explain their CDs PL using molecular state.[31] These claimed the precursor/precursor fragment is on the surface of CDs. While there is strong evidence for this theory in some CDs systems, it is certainly limited based on the precursor and cannot completely explain

the excitation-dependent emission CDs usually possess. The third and most common theory that is used is the surface state-controlled PL. The frequent use of this explanation has caused the general acceptance of this theory for the PL mechanism of CDs.[30] However, very infrequently is the origin of this theory traced back to solid-state physics and semiconductors. Additionally, when surface-state controlled PL is offered as an explanation for CDs PL, it is not stated if the concept can be directly applied to CDs or if modifications are necessary. In view of this, a greater understanding of surface states is needed to understand CDs' PL.

4.2 Surface states in semiconductors

The concept of surface state controlled electronic properties/structure has been developed by solid-state physicists to describe the electronic properties of semiconductors.[118, 119] This concept was first applied to CDs in 2006.[8] Surface states in semiconductors are often classified into intrinsic and extrinsic surface states. Intrinsic surface states are electronic states which result in the termination of the elemental lattice at the semiconductor/vacuum interface. Intrinsic surface states are modeled computationally as Shockley or Tamm states. Shockley surface states are modeled using a "nearly-free electron" model and can be used accurately for narrow gap semiconductors (bandgaps approximately 1–2 eV). Tamm states are modeled using the "tight-bound" approach and are expressed as a linear combination of atomic orbitals (LCAO). These states are valuable for broad gap semiconductors (2–4 eV bandgaps).[120]

Extrinsic surface states in semiconductors can arise from defects in the crystal lattice at the surface, adsorbates to the semiconductor, and interfaces between two materials. Extrinsic surface states are much more difficult to characterize and model than intrinsic surface states. Additionally, these surface states are often unique for a particular system, depending on the atoms and structure present, and the defects in that structure.[121] While it is not always explicitly stated, extrinsic surface states are claimed to control the PL of CDs in many papers. To understand what has been reported for CDs' PL mechanism, attention will now be turned to the application of this concept to CDs.

4.3 Recent developments in understanding carbon dots photoluminescence

Surface state-controlled PL in CDs was first suggested by Sun et al.[8] in 2006 for CDs prepared by laser ablation and passivated by PEG_{1500N}. They proposed surface energy traps which are stabilized by passivation with PEG_{1500N}. Since then there has been many developments and variations of this idea. In 2015, Ding et al.[122] produced CDs from p-phenylenediamine and urea and separated different fractions through column chromatography. They found the wavelength of PL increased with the increasing degree of oxidation (as seen by FTIR and XPS). They attribute the PL of CDs to conjugated sp^2 carbons on the surface of CDs whose bandgap can reduced by the degree of oxidative surface defects as shown in figure 10. Modeling of graphene oxide through density functional theory supports the distortion of the electronic environment by oxidation on sp^2 carbons.[123]

Zhang et al.[124] also attributed excitation-dependent emission to surface oxidation. They prepared CDs (CD1) using an electrochemical preparation from urea, graphite, and NaOH. They also prepared CDs (CD2) from citric acid and trisaminomethane using a microwave preparation. Both CD1 and CD2 displayed blue PL, but CD1 possessed excitation wavelength-independent emission, whereas CD2 was dependent on excitation wavelength. XPS atomic ratio showed that CD2 possessed much higher surface oxygen levels. The authors conclude CD2 has many different oxygen functionalities in the n-π^* region of CDs absorption (ca. 350 nm) which creates different surface states resulting in the shifting emission of CD2. Both preceding studies use surface oxidation to explain excitation-dependent emission as well as the PL color of CDs. However, the shifting which results from Ding et al.[108] work spans a much larger region (blue to red emission) than does the work by Zhang et al.[110] (just blue emission). This could indicate both the complexity of the PL process in CDs as well as the heavy dependence of CDs' optical properties on precursor and preparation method.

Other atoms have been hypothesized to influence CDs PL color. Han et al.[125] used a hydrothermal method with hydroquinone and EDA to generate CDs which could be separated via silica-gel chromatography to give blue, green, and yellow emissive CDs fractions. They determined the PL color to be related to the surface state due to the influences of pH and solvent on emission of the three fractions. Through XPS analysis of the N1s binding energies, they were able to show the C=N percentage increased with the increasing wavelength of emission. Other nitrogen groups (-NH_2 and C-N-C) displayed no correlation with PL color of CDs. As further evidence for imine-controlled emission, the excitation spectrum of CDs overlapped with n-π^* transition for C=N in the absorbance spectrum. Their concluding hypothesis states that imine groups on the surface of CDs creates surface defects which introduces energy levels into the bandgap of CDs, thus reducing the energy of the emitted PL.[126]

Recently, Yuan et al.[127] compared the optical and surface properties of 4 different CDs (figure 11a). The color of each CDs image in figure 11a represents the PL spectra of the produced CDs. When they compared the nitrogen content of the four CDs (figure 11d), they could see clear differences for type and amount of nitrogen functionality in each sample. They attribute the red emission to the distortion of p-phenylenediamine. When ethylenediamine (EDA) is introduced into the preparation the amount of pyrrolic and amino nitrogen decreases and the amount of pyridinic nitrogen increases. This leads to the conclusion that pyridinic nitrogen is responsible for the green emission. When PEI is used as a precursor, blue emission is again seen and the pyrrolic nitrogen increases, which suggests the blue emission and pyrrolic nitrogen are related. These relationships are further confirmed by the presence of red and blue emission in CDs prepared from proline. Based on these observations, the authors suggest a representative structure for each CDs and create an energy level diagram to illustrate the effect of surface nitrogen functionalization on the bandgap of CDs (figure 11 B,C).

Liu et al.[128] used a microwave reaction with formamide and ortho, meta, and para-phenylenediamine separately to form o-CDs, m-CDs, and p-CDs. Surprisingly, the PL color did not follow the isomeric trend as the CDs possessed yellow, blue, and orange PL

emission, respectively. All CDs also displayed excitation-independent emission, which they attribute to uniformity of structure. From surface analysis of the CDs through XPS they see varying degrees of heteroatoms present. It was found that as C=O/CONH content increased so did the wavelength of emission. This was once again attributed to oxidative surface defects reducing the bandgap in the CDs. Another trend was also observed between non-amino nitrogen content (pyridinic and pyrrolic nitrogen) and QY. The determined QY for p-CDs, m-CDs, and o-CDs was 7.5, 14.3, and 45.0%, respectively. Coinciding with this trend they saw an increase in the non-amino nitrogen content, which they attribute to the increase in the conjugated structure at the CDs surface which promoted radiative recombination. As previously discussed, nitrogen doping is well known to increase the QY for CDs, but this study provides more information on the specific groups which increase QY.

Due to the increasing success of surface state theory to explain CDs PL properties it has become much more common than quantum confinement and molecular state. Quantum confinement is occasionally used to explain the PL of CDs, but it is often used in conjunction with another concept such as surface state.[2, 29, 129, 130] In 2018, Liu et al.[130] prepared CDs from a perylene derivative and triethylamine and separated the resulting mixture using column chromatography. This yielded 25 fractions with emission ranging from blue to the near infrared. Their characterization showed a rough correlation between size, polarity, and emission wavelength. This led the authors to conclude that the emission of the CDs is roughly adjusted by quantum confinement effects and more subtly adjusted by surface states. In recent years, most researchers have not used quantum confinement as the sole factor for CDs PL mechanism and many studies' data do not support a size-dependent emission for CDs.

Molecular state is also used occasionally, but it is clear that the concept cannot be applied to all CDs systems. CDs prepared from citric acid and a nitrogen dopant and also precursors which already possess fluorescence are the limit of molecular states' ability to explain CDs PL.[31, 131, 132] Based on the trends in recent CDs literature, it appears that a surface state controlled PL will be investigated more deeply in the future.

5. Developments in elucidation of carbon dots' core structure

Similar to graphene quantum dots (GQDs) and polymer dots (PDs), CDs are known for core-shell structure. However, in term of chemical structure, they are distinct. To be specific, GQDs' core consists of simply single or few layers of graphene, which are connected to chemical groups on the edge to form the shell of GQDs.[133] PDs that result from the assembly/aggregation or cross-link of non-conjugated polymers are composed of carbon core and polymer chains as the shell.[2] In comparison, CDs' structure is the combination of a sp^3-hybridized matrix of oxygen/nitrogen-containing surface functional groups (defect states) and core (intrinsic states).[134] The formation of CDs is a nucleation process with a gradual growth of core and a "self-passivated" shell comprising functional groups.[135] In 2018, Ren et al. reported that both core and surface electronic states of CDs contributed to the optical properties and electronic acceptor levels while the chemical nature of the surface groups determined the hydrogen bonding behavior of the CDs.[136] It arouses much attention to the functions of the core and the surface chemistry of the shell of CDs.

The surface chemistry of CDs shell consists of the chemical structure and functions of the shell. As to the chemical structure, in the shell of CDs, there are various connected or modified functional groups such as oxygen-, amino-based groups or polymer chains, etc., which depends on the starting materials or dopant species and were usually characterized by FTIR and XPS.[2] In addition, there ought to be abundant C=C and C=O conjugate structures that were often observed from UV/vis spectra of CDs.[94] Regarding the function, the surface chemistry of shell controls the stability of CDs aqueous solution. The surface zeta potential can reveal the strength of electrostatic repulsion amongst CDs. Specially, the electrostatic repulsion gets weaker when the zeta potential value is smaller, which suggests the less stability of the CDs aqueous solution and ease to aggregate. In addition, the composition (functional groups) of the shell is vital to subsequent functionalization required for many applications.[137–139] Furthermore, the shell involves in the unique optical properties and electron donor/acceptor of CDs. For example, CDs have pH-dependent PL, which has been widely reported, and the PL can be monitored by different pH to study the effect of the surface groups on optical properties.[140, 141] Also, depending on the surface moieties, the surface-related electronic acceptor levels can be modulated, which may affect PL properties of CDs.[136]

However, even though the shell is widely investigated since the discovery of CDs due to the excellent PL, the core study was not begun until 2008.[142] In 2008, Bourlinos et al. put forward that single CD should have a carbogenic core, which is composed of carbonized intermediates with a highly defected structure of co-existing aromatic and aliphatic regions.[142] However, due to the highly photoluminescent nature, further characterization regarding the structure was limited then and is still a problem presently. The core is often considered carbogenic without deeper understanding even in many recent research articles.[143] Therefore, it is necessary to summarize the development in the understanding of the core to date as well as the role it plays in the PL of CDs.

Owing to the recent wide investigation, current theories points out that there are two types of cores of CDs, graphitic crystalline and amorphous cores, based on the degree of the presence of sp^2 carbon in the core.[94] Among them, the graphitic crystalline core has been more reported,[144, 145] and the cores are small in size (2–3 nm) with a lattice spacing of ~0.2 nm.[146] However, sometimes the core exists in the form of two types of cores. For example, Galan's group reported a type of CDs through a 3 min synthesis contained an sp^3-enriched crystalline core and the abundant sp3 carbon induced the amorphousness.[147] Moreover, the type of cores depends on the synthetic approaches and can be converted between each other.[148] In general, reaction temperatures above 300 °C lead to significant graphitization while those below lead to amorphous core,[149] unless sp^2/sp hybridized carbon was present in the precursor.[150] For example, many early synthetic approaches of CDs contained the fragmentation of the macroscopic carbon source, which caused or maintained the crystalline organization in the core of synthesized CDs.[151]

However, until now, there is still no direct observable result of the core in CDs and the present theory merely results from the evidence according to various characterization techniques such as NMR, XPS, TEM, XRD, and Raman spectroscopy.

TEM, XRD and Raman spectroscopy are direct characterization methods. High-resolution TEM provides a straightforward route to confirm the presence of CDs. Some researchers observed graphitic crystalline structure in Nanoarticles by high-resolution TEM and it was believed to be the core of CDs.[152] XRD is also an important technique to help detect the morphology of the CDs core. For example, Martindale et al.[148] mentioned in their work the powder XRD pattern of CDs core shows a broad peak centered at 27.0° 2θ consistent with a nanocrystalline graphitic structure. As to Raman spectroscopy, a G band indicates the first-order Raman band of all sp^2 hybridized carbon materials while a D band is a defect activated band in sp^2 hybridized carbon materials. Herein, in the core study, the ratio of spectral intensities of D and G bands (ID/IG) reflects the defect density of the CDs core. Hola et al.[123] synthesized CDs from lauryl (dodecyl) gallate (LG27), propyl gallate (PG27), and methyl gallate (MG27) with a decreasing ID/IG, which was explained by the effect of decreasing alkyl-chain length on the carbogenic core. In addition, upon observing the identical emission spectra of CDs from LG27 and LG 270, they hypothesized a direct excitonic recombination from the core rather than the surface is the major PL emission source. However, the PL mechanism is always under debate and the conclusion above probably only works for their own CDs since it contradicts many other research results as previously discussed. For example, Nguyen et al.[153] supported that the PL of CDs resulted from the abundant surface functional groups rather than the core.

In addition, NMR, XPS and TGA are used as the supplementary characterization methods to determine the general structure and properties of the core of CDs.[154] In 2013, Giannelis and co-workers[155] performed the structural analysis of the surface modifier on three types of CDs by using 1D or 2D high resolution NMR spectroscopy in solution. However, they didn't observe any ^1H NMR signal that could be assigned to the CDs core, which was consistent with the core carbonization hypothesis from Bourlinos et al.[142, 156] So, they proposed a solid-state NMR is needed in the future to fully confirm the core carbonization hypothesis and study the chemical structure of the core. Based on high-resolution XPS measurement, for N-doped CDs the core is not purely composed of carbon.[157] Doped-N was also a contributor to the formation of core in cyclic form including pyrrolic, graphitic and pyridinic nitrogen resulting in a strong electron-withdrawing ability within the conjugated C plane. This significance of nitrogen in the construction of CDs was supported by Hill et al. In Hill et al.'s work[126], the morphology of the core of CDs can be tuned by surface passivating agent. The longer linker could help increase the size of core but also might induce the disorder and lower graphitization degree. And the incorporation of nitrogen could also improve the PL by enhancing the core emission, which was later reported by Gregorkiewicz and co-workers.[143] Also, in Weijan et al.'s work, [157] they performed TGA on both CDs and N-doped CDs. Meanwhile, the TGA measurements exhibited distinct stages for the surface and core of CDs.

The core is closely correlated to the optical properties of CDs. As is known the UV/vis spectra of typical CDs have two typical absorption peaks at around 250 and 350 nm, which could be assigned to π-π^* and n-π^* transitions of C=C and C=O, respectively, in the core of CDs.[158, 159] As discussed previously, the PL of CDs is usually believed to originate from the radiative recombination of excitons in core (carbon-core states) and surface electronic states, molecular states, surface functional groups and surface energy traps. Among them molecular

states and carbon-core states were demonstrated for the first time by Giannelis and co-workers[160] in CDs prepared from citric acid and ethanolamine, and the radiative recombination of excitons in the surface states are more tunable.[161] Later, the presence of three different emission centers including molecular states, aromatic domain states, and carbon-core states was shown by Shamsipur et al.[134] in CDs synthesized through pyrolysis of citric acid and ethylenediamine for the first time. And they discussed that the main PL of citric acid-based CDs derives from the molecular states rather than the carbon-core states, which results in lower photostability and higher PL reduction. Meanwhile, compared to the molecular states, the carbon-core states usually emit at shorter wavelengths and exhibit much lower PL QY.[160] Also, more uniform functional groups on a highly crystalline core result in higher PL QY. On the contrary, lower QY can be observed for CDs with more traps and fewer surface functional groups.[153] Therefore, even though the surface state theory is a dominant theory for the PL mechanism, we can't ignore the contribution of the core in the PL emission especially in the short-wavelength region. According to Gregorkiewicz and co-workers,[122] the core related PL emission results from the π-π^* transition of sp^2 clusters assisted by the quantum confinement effect and the emission at longer wavelengths is known to be related to the hybridized oxygen functional groups with the core.[162]

The PL mechanism can also be interpreted by the electronic transition involving the coupling of the core and surface states.[145] As is concluded from Yu et al.'s work, both surface states and carbon core are critical for the regulation of PL emission since the band gap of surface states (4.5 eV) is narrower than that of the core (5.0 eV).[163] In addition, the oxygen and nitrogen elements and related chemical bonds will produce impurity levels in the band gap, which leads to the change of excitation and emission spectra of CDs. As shown in Figure 12, there may be an energy transfer process between the carbon core and the surface state. The CDs display five emission bands centered at 305, 355, 410, 445, and 500 nm, which are correlated with the electron transition at intrinsic C (4.1 eV), graphitic N (3.5 eV), pyridine N (3.0 eV), amino N (2.8 eV), and C=O (2.5 eV) related levels, respectively. With the development of characterization methods, probably one day we will be able to clearly observe and accurately separate the core from the shell. Then many ambiguous questions can get a solid answer, such as the PL mechanism and the structure of the core.

6. Conclusion and Future Perspectives

Some important optical properties have been discussed regarding CDs, namely QY and PL decay lifetime. These are important parameters in assessing the utility of CDs in application such as imaging and sensing. Carbon sources used for preparing CDs have ranged from graphite, proteins, small molecules, and food products. Citric acid is the most commonly used precursor at the moment and has produced CDs with high QYs and long PL decay lifetime, but many different carbon sources have shown promising properties. A more significant factor appears to be heteroatom doping with nitrogen, sulfur, boron, or phosphorous. The effect of heteroatom doping has been shown many times to have a positive effect on both QY and PL lifetime and appears to be a significant factor in determining the optical properties. Additionally, the method used to prepare CDs influences the optical properties of CDs. Thermal methods are most often used and often give favorable properties,

but microwave methods have also given rise to CDs with high QYs and long PL lifetimes as well. Top-down methods such as laser ablation or electrochemical methods do not often produce CDs which are used in applications such as sensing and imaging, as the QY from these CDs tends to be lower. In contrast, the obtained PL decay lifetime doesn't have an obvious enhancement regarding either "top-down" or "bottom-up" approach.

Additionally, the PL mechanism of CDs has been discussed, mainly for the surface state-controlled PL. These have been shown to involve oxygen or nitrogen functionalities which create surface defects on the surface of CDs. These defects can modulate the color of PL as well as create an heterogenous electronic environment resulting in excitation wavelength-dependent emission.

The core of CDs remains unclear, but many works have been presented to support graphitic, crystalline, and amorphous cores. The discord in the literature reflects the variation in CDs properties based on preparation methods. New characterization methods are needed to provide clarity in this area.

Moving forward it is important to ensure that all literature values for QY of CDs are reliable. As previously stated, CDs possess favorable optical properties and much work is currently being done to realize their full potential. Proper selection of a QY standard and correct experimental techniques are essential to correctly reporting QYs. When this is not done, and exaggerated values are reported, reproducibility issues often occur which casts doubt on any high QYs reported in literature for CDs. Also, PL decay life is an important property that should not be missing for the analysis to understand the PL mechanism of CDs and broadening their application.

Further improvement is needed in the QYs of CDs with long wavelength emission. High values, above 90%, have been reported for emission in the blue region of light, but QY values measured at longer wavelengths are often low or are compromised due to dubious QY standard choice.[122, 164] There is great potential for applications in bio-imaging to avoid the autofluorescence of tissues and other areas for CDs which possess emission above 650 nm, in the red or infrared region. Compared to the QY measurement, PL decay lifetime hasn't been outlined and it is always under 20 ns, which remains to be enhanced.

As mentioned for the optical parameters above, the wide diversity of preparation methods and precursors creates difficulty in illuminating the PL mechanism and core structure of CDs. In the future it will be important to develop new characterization in these areas, as well as to rigorously compare new data with what has been previously reported. At the moment it is unclear if there are different processes occurring for different preparation methods (top-down versus bottom-up) or different precursors. New results on these topics should be compared to previous results for similar systems.

The great improvements made in the optical properties of CDs in recent years have been extensively discussed. In the areas of PL decay lifetime, QY reproducibility, long wavelength emission of CDs, and the understanding of PL mechanism and core structure, there is still more room for improvement. However, CDs have shown great potential in the

areas of imaging and sensing, and their applications will continue to expand in the coming years.

Supplementary Material

Refer to Web version on PubMed Central for supplementary material.

Acknowledgment

Funding sources (R.M.L.) include the National Science Foundation through grant 1809060 and the National Institute of Health through grant R21AR072226.

References

1. Xu X, Ray R, Gu Y, Ploehn HJ, Gearheart L, Raker K and Scrivens WA, J. Am. Chem. Soc, 2004, 126, 12736–12737. [PubMed: 15469243]
2. Zhu S, Song Y, Zhao X, Shao J, Zhang J and Yang B, Nano Res, 2015, 8, 355–381.
3. Yang S-T, Cao L, Luo PG, Lu F, Wang X, Wang H, Meziani MJ, Liu Y, Qi G and Sun Y-P, J. Am. Chem. Soc, 2009, 131, 11308–11309. [PubMed: 19722643]
4. Yang S-T, Wang X, Wang H, Lu F, Luo PG, Cao L, Meziani MJ, Liu J-H, Liu Y and Chen M, The J. Phys. Chem. C, 2009, 113, 18110–18114.
5. Qu K, Wang J, Ren J and Qu X, Chem. Eur. J, 2013, 19, 7243–7249. [PubMed: 23576265]
6. Lin Z, Xue W, Chen H and Lin J-M, Anal. Chem, 2011, 83, 8245–8251. [PubMed: 21899286]
7. Ding C, Zhu A and Tian Y,Acc. Chem. Res, 2013, 47, 20–30. [PubMed: 23911118]
8. Sun Y-P, Zhou B, Lin Y, Wang W, Fernando KS, Pathak P, Meziani MJ, Harruff BA, Wang X and Wang H, J. Am. Chem. Soc, 2006, 128, 7756–7757. [PubMed: 16771487]
9. Luo PG, Sahu S, Yang S-T, Sonkar SK, Wang J, Wang H, LeCroy GE, Cao L and Sun Y-P, J. Mater. Chem. B, 2013, 1, 2116–2127.
10. Li S, Wang L, Chusuei CC, Suarez VM, Blackwelder PL, Micic M, Orbulescu J and Leblanc RM, Chem. Mater, 2015, 27, 1764–1771.
11. Małolepszy A, Błonski S, Chrzanowska-Giżyńska J, Wojasiński M, Płocinski T, Stobinski L and Szymanski Z, J. Appl. Phys. A, 2018, 124, 282–288.
12. Wang Y, Wang K, Han Z, Yin Z, Zhou C, Du F, Zhou S, Chen P and Xie Z, J. Mater. Chem. C, 2017, 5, 9629–9637.
13. Zuo P, Lu X, Sun Z, Guo Y and He H, Microcim. Acta, 2016, 183, 519–542.
14. Xu Q, Pu P, Zhao J, Dong C, Gao C, Chen Y, Chen J, Liu Y and Zhou H, J. Mater. Chem. A, 2015, 3, 542–546.
15. Yang S, Sun J, Li X, Zhou W, Wang Z, He P, Ding G, Xie X, Kang Z and Jiang M, J. Mater. Chem. A, 2014, 2, 8660–8667.
16. Dong Y, Pang H, Yang HB, Guo C, Shao J, Chi Y, Li CM and Yu T, Angew. Chem. Int. Ed, 2013, 52, 7800–7804.
17. Choi Y, Kang B, Lee J, Kim S, Kim GT, Kang H, Lee BR, Kim H, Shim S-H and Lee G, Chem. Mater, 2016, 28, 6840–6847.
18. Qu D, Zheng M, Zhang L, Zhao H, Xie Z, Jing X, Haddad RE, Fan H and Sun Z, Sci. Rep, 2014, 4, 5294–5304. [PubMed: 24938871]
19. Li X, Zhang S, Kulinich SA, Liu Y and Zeng H, Sci. Rep, 2014, 4, 4976–4983.
20. Liu L, Li Y, Zhan L, Liu Y and Huang C, Sci. China Chem, 2011, 54, 1342–1347.
21. Dong Y, Pang H, Yang HB, Guo C, Shao J, Chi Y, Li CM and Yu T, Angew. Chem. Int. Ed, 2013, 52, 7800–7804.
22. Zheng C, An X and Gong J, RSC Adv, 2015, 5, 32319–32322.
23. Kalytchuk S, Poláková K, Wang Y, Froning JP, Cepe K, Rogach AL and Zbořil R, ACS Nano, 2017, 11, 1432–1442. [PubMed: 28125202]

24. Nguyen V, Si J, Yan L and Hou X, Carbon, 2015, 95, 659–663.
25. Song Y, Zhu S, Shao J and Yang B, J. Polym. Sci. A, 2017, 55, 610–615.
26. Hill SA, Benito-Alifonso D, Davis SA, Morgan DJ, Berry M and Galan MC, Sci. Rep, 2018, 8, 12234–12243. [PubMed: 30111806]
27. Chen D, Gao H, Chen X, Fang G, Yuan S and Yuan Y, ACS Photonics, 2017, 4, 2352–2358.
28. Shen Y, Liang Y, Wang Y, Liu C and Ren X,J. Nanoart. Res, 2018, 20, 229–238.
29. Liu W, Li C, Sun X, Pan W, Yu G and Wang J, Nanotechnology, 2017, 28, 485705–485717. [PubMed: 28961145]
30. Zhu S, Song Y, Wang J, Wan H, Zhang Y, Ning Y and Yang B, Nano Today, 2017, 13, 10–14.
31. Pan X, Zhang Y, Sun X, Pan W, Yu G, Zhao Q and Wang J, J. Lumin, 2018, 204, 303–311.
32. Gharat PM, Chetodhil J, Srivastava AP, Praseetha P, Pal H and Choudhury SD, Photoch. Photobio. Sci, 2019, 18, 110–119.
33. Martindale BC, Hutton GA, Caputo CA, Prantl S, Godin R, Durrant JR and Reisner E, Angew. Chem. Int. Ed, 2017, 56, 6459–6463.
34. Sciortino L, Sciortino A, Popescu R, Schneider R, Gerthsen D, Agnello S, Cannas M and Messina F, J. Phys. Chem. C, 2018, 122, 19897–19903.
35. Lu S, Sui L, Wu M, Zhu S, Yong X and Yang B, Adv. Sci, 2019, 6, 1801192–1801199.
36. Wang J and Qiu J, J. Mater. Sci, 2016, 51, 4728–4738.
37. Zhou J, Zhou H, Tang J, Deng S, Yan F, Li W and Qu M, Microcim. Acta, 2017, 184, 343–368.
38. Namdari P, Negahdari B and Eatemadi A, Biomed. Pharmacother, 2017, 87, 209–222. [PubMed: 28061404]
39. Zu F, Yan F, Bai Z, Xu J, Wang Y, Huang Y and Zhou X, Microcim. Acta, 2017, 184, 1899–1914.
40. Yan F, Jiang Y, Sun X, Bai Z, Zhang Y and Zhou X, Microcim. Acta, 2018, 185, 424.
41. Liu ML, Chen BB, Li CM and Huang CZ, Green Chem, 2019, in press.
42. Fery-Forgues S and Lavabre D, J. Chem. Educ, 1999, 76, 1260.
43. Olmsted J, J. Phys. Chem, 1979, 83, 2581–2584.
44. Sun Y-P, Wang X, Lu F, Cao L, Meziani MJ, Luo PG, Gu L and Veca LM, J. Phys. Chem. C, 2008, 112, 18295.
45. Gonçalves H, Jorge PA, Fernandes J and da Silva JCE, Sens. Actuators B Chem, 2010, 145, 702–707.
46. Qu S, Liu X, Guo X, Chu M, Zhang L and Shen D, Adv. Funct. Mater, 2014, 24, 2689–2695.
47. Yuan YH, Liu ZX, Li RS, Zou HY, Lin M, Liu H and Huang CZ, Nanoscale, 2016, 8, 6770–6776. [PubMed: 26955862]
48. Wang J, Zhang P, Huang C, Liu G, Leung KC-F and Wáng YXJ, Langmuir, 2015, 31, 8063–8073. [PubMed: 26135003]
49. Yu S, Chen K, Wang F, Zhu Y and Zhang X, Luminescence, 2017, 32, 970–977. [PubMed: 28139046]
50. Kudr J, Richtera L, Xhaxhiu K, Hynek D, Heger Z, Zitka O and Adam V, Biosens. Bioelectron, 2017, 92, 133–139. [PubMed: 28213325]
51. Roshni V and Divya O, Curr. Sci, 2017, 112, 385–390.
52. Li J-Y, Liu Y, Shu QW, Liang J-M, Zhang F, Chen X-P, Deng X-Y, Swihart MT and Tan KJ, Langmuir, 2017, 33, 1043–1050. [PubMed: 28064483]
53. Dong Y, Shao J, Chen C, Li H, Wang R, Chi Y, Lin X and Chen G, Carbon, 2012, 50, 4738–4743.
54. Song Y, Zhu S, Zhang S, Fu Y, Wang L, Zhao X and Yang B, J. Mater. Chem. C, 2015, 3, 5976–5984.
55. Shi L, Yang JH, Zeng HB, Chen YM, Yang SC, Wu C, Zeng H, Yoshihito O and Zhang Q, Nanoscale, 2016, 8, 14374–14378. [PubMed: 27426926]
56. Li L, Lu C, Li S, Liu S, Wang L, Cai W, Xu W, Yang X, Liu Y and Zhang R, J. Mater. Chem. B, 2017, 5, 1935–1942.
57. Chandra S, Mahto TK, Chowdhuri AR, Das B and S. k. Sahu, Sens. Actuators B Chem, 2017, 245, 835–844.

58. Yang Z, Xu M, Liu Y, He F, Gao F, Su Y, Wei H and Zhang Y, Nanoscale, 2014, 6, 1890–1895. [PubMed: 24362823]
59. Wang H, Gao P, Wang Y, Guo J, Zhang K-Q, Du D, Dai X and Zou G, APL Mater, 2015, 3, 086102–086108.
60. Zhou Y, Desserre A, Sharma SK, Li S, Marksberry M, Chusuei C, Blackwelder P and Leblanc RM, ChemPhysChem, 2017, 18, 890–897. [PubMed: 28170162]
61. Ji Y, Zhou Y, Waidely E, Desserre A, Marksberry MH, Chusuei CC, Dar AA, Chat OA, Li S and Leblanc RM, Inorg. Chim. Acta, 2017, 468, 119–124.
62. Zhou Y, Liyanage P, Geleroff D, Peng Z, Mintz K, Hettiarachchi S, Pandey R, Chusuei C, Blackwelder P and Leblanc R, ChemPhysChem, 2018, 19, 2589–2597. [PubMed: 29856902]
63. Wen Z-H and Yin X-B, RSC Adv, 2016, 6, 27829–27835.
64. Parvin N and Mandal TK, Microcim. Acta, 2017, 184, 1117–1125.
65. Krysmann MJ, Kelarakis A, Dallas P and Giannelis EP, J. Am. Chem. Soc, 2011, 134, 747–750. [PubMed: 22201260]
66. Niu W-J, Li Y, Zhu R-H, Shan D, Fan Y-R and Zhang X-J, Sens. Actuators B Chem, 2015, 218, 229–236.
67. Tao S, Song Y, Zhu S, Shao J and Yang B, Polymer, 2017, 116, 472–478.
68. Yang Y, Kong W, Li H, Liu J, Yang M, Huang H, Liu Y, Wang Z, Wang Z, Sham T-K, Zhong J, Wang C, Liu Z, Lee S-T and Kang Z, ACS Appl. Mater. Interfaces, 2015, 7, 27324–27330. [PubMed: 26593857]
69. Mintz KJ, Mercado G, Zhou Y, Ji Y, Hettiarachchi SD, Liyanage PY, Pandey RR, Chusuei CC, Dallman J and Leblanc RM, Colloids Surf. B, 2019, 176, 488–493.
70. Xu Q, Kuang T, Liu Y, Cai L, Peng X, Sreeprasad TS, Zhao P, Yu Z and Li N, J. Mater. Chem. B, 2016, 4, 7204–7219.
71. Xu Q, Li B, Ye Y, Cai W, Li W, Yang C, Chen Y, Xu M, Li N and Zheng X, Nano Res, 2017, 11, 3691–3701.
72. Xu Q, Su R, Chen Y, Theruvakkattil Sreenivasan S, Li N, Zheng X, Zhu J, Pan H, Li W and Xu C, ACS Appl. Nanomater, 2018, 1, 1886–1893.
73. Hu L, Sun Y, Li S, Wang X, Hu K, Wang L, Liang X.-j. and Wu Y, Carbon, 2014, 67, 508–513.
74. Yang C, Thomsen RP, Ogaki R, Kjems J and Teo BM, J. Mater. Chem. B, 2015, 3, 4577–4584.
75. Yang X, Wang Y, Shen X, Su C, Yang J, Piao M, Jia F, Gao G, Zhang L and Lin Q, J. Colloid Interface Sci, 2017, 492, 1–7. [PubMed: 28068539]
76. Yang Z-C, Wang M, Yong AM, Wong SY, Zhang X-H, Tan H, Chang AY, Li X and Wang J, Chem. Commun, 2011, 47, 11615–11617.
77. Nandi S, Malishev R, Kootery KP, Mirsky Y, Kolusheva S and Jelinek R, Chem. Commun, 2014, 50, 10299–10302.
78. Song Y, Zhu C, Song J, Li H, Du D and Lin Y, ACS Appl. Mater. Interfaces, 2017, 9, 7399–7405. [PubMed: 28134510]
79. Xu S, Liu Y, Yang H, Zhao K, Li J and Deng A, Anal. Chim. Acta, 2017, 964, 150–160. [PubMed: 28351631]
80. Yang J, Chen W, Liu X, Zhang Y and Bai Y, Mater. Res. Bull, 2017, 89, 26–32.
81. Ghosh SA, Kumar VB, Fixler D, Dubinsky Z, Gedanken A and Iluz D, Algal Res, 2017, 23, 161–165.
82. Zhou J, Sheng Z, Han H, Zou M and Li C, Mater. Lett, 2012, 66, 222–224.
83. De B and Karak N, RSC Adv, 2013, 3, 8286–8290.
84. Wang L and Zhou HS, Anal. Chem, 2014, 86, 8902–8905. [PubMed: 25181643]
85. Mandani S, Dey D, Sharma B and Sarma TK, Carbon, 2017, 119, 569–572.
86. Liu Y, Liu Y, Park M, Park S-J, Zhang Y, Akanda MR, Park B-Y and Kim HY, Carbon Lett, 2017, 21, 61–67.
87. Baker SN and Baker GA, Angew. Chem. Int. Ed, 2010, 49, 6726–6744.
88. Elangovan M, Day R and Periasamy A, J. Microsc, 2002, 205, 3–14. [PubMed: 11856376]

89. Ryu J, Kang U, Kim J, Kim H, Kang JH, Kim H, Sohn DK, Jeong J.-h., Yoo H and Gweon B, Biomed. Opt. Express, 2018, 9, 3449–3463. [PubMed: 29984109]
90. Narayanan R, Deepa M and Srivastava AK, J. Mater. Chem. A, 2013, 1, 3907–3918.
91. Rahul C, Sebastian R, Mark M, Yuri MS, Ignacy G, Julian B, Zygmunt G and Rafal F, Methods Appl. Fluoresc, 2016, 4, 047001–047008. [PubMed: 28192308]
92. Li H, Sun C, Vijayaraghavan R, Zhou F, Zhang X and MacFarlane DR, Carbon, 2016, 104, 33–39.
93. Berezin MY and Achilefu S, Chem. Rev, 2010, 110, 2641–2684. [PubMed: 20356094]
94. Zhou Y, Sharma S, Peng Z and Leblanc R, Polymers, 2017, 9, 67–86.
95. Yang Z, Li Z, Xu M, Ma Y, Zhang J, Su Y, Gao F, Wei H and Zhang L, Nano-Micro Lett, 2013, 5, 247–259.
96. Ghamsari MS, Bidzard AM, Han W and Park H-H, Nano, 2016, 10, 026028–026028.
97. Zhou Y, Desserre A, Sharma SK, Li S, Marksberry MH, Chusuei C, Blackwelder PL and Leblanc RM, ChemPhysChem, 2017, 18, 890–897. [PubMed: 28170162]
98. Wang Q, Zhang C, Shen G, Liu H, Fu H and Cui D, J. Nanobiotechnology, 2014, 12, 58–69. [PubMed: 25547381]
99. Chowdhury D, Gogoi N and Majumdar G, RSC Adv, 2012, 2, 12156–12159.
100. Jaiswal A, Ghosh SS and Chattopadhyay A, Chem. Commun, 2012, 48, 407–409.
101. Liu H, Ye T and Mao C, Angew. Chem. Int. Ed, 2007, 46, 6473–6475.
102. Mohanty B, Anita KV, Claesson P and Bohidar HB, Nanotechnology, 2007, 18, 445102–445110.
103. Kumar P and Bohidar HB, J. Lumin, 2013, 141, 155–161.
104. Wang H, Sun P, Cong S, Wu J, Gao L, Wang Y, Dai X, Yi Q and Zou G, Nanoscale Res. Lett, 2016, 11, 27–32. [PubMed: 26781285]
105. Liu J, Liu X, Luo H and Gao Y, RSC Adv, 2014, 4, 7648–7654.
106. Li X, Zhang S, Kulinich SA, Liu Y and Zeng H, Sci. Rep, 2014, 4, 4976–4983.
107. Rice KM, Walker EM, Wu M, Gillette C and Blough ER, J. Prev. Med. Public Health, 2014, 47, 74–83. [PubMed: 24744824]
108. Sachdev A, Matai I and Gopinath P, RSC Adv, 2014, 4, 20915–20921.
109. Jiang K, Wang Y, Gao X, Cai C and Lin H, Angew. Chem. Int. Ed, 2018, 57, 6216–6220.
110. Jiang K, Wang Y, Cai C and Lin H, Adv. Mater, 2018, 30, 1800783–1800790.
111. Long P, Feng Y, Cao C, Li Y, Han J, Li S, Peng C, Li Z and Feng W, Adv. Funct. Mater, 2018, 28, 1800791–1800800.
112. Gao Y, Han H, Lu W, Jiao Y, Liu Y, Gong X, Xian M, Shuang S and Dong C, Langmuir, 2018, 34, 12845–12852. [PubMed: 30346780]
113. Li Q, Zhou M, Yang M, Yang Q, Zhang Z and Shi J, Nature Commun, 2018, 9, 734–738. [PubMed: 29467414]
114. Tan J, Ye Y, Ren X, Zhao W and Yue D, J. Mater. Chem. C, 2018, 6, 7890–7895.
115. Alivisatos AP, Science, 1996, 271, 933–937.
116. Zhu S, Zhao X, Song Y, Lu S and Yang B, Nano Today, 2016, 11, 128–132.
117. Dhenadhayalan N, Lin K-C, Suresh R and Ramamurthy P, J. Phys. Chem. C, 2016, 120, 1252–1261.
118. Moll JL, Physics of Semiconductors, McGraw Hill, 1964.
119. McKelvey JP, Solid state and semiconductor physics, Harper and Row, 1966.
120. Colinge J-P and Colinge CA, Physics of semiconductor devices, Springer Science & Business Media, 2005.
121. Dimitrijev S, Principles of semiconductor devices, Oxford University Press, USA, 2006.
122. Ding H, Yu S-B, Wei J-S and Xiong H-M, ACS Nano, 2015, 10, 484–491. [PubMed: 26646584]
123. Chien CT, Li SS, Lai WJ, Yeh YC, Chen HA, Chen IS, Chen LC, Chen KH, Nemoto T and Isoda S, Angew. Chem. Int. Ed, 2012, 51, 6662–6666.
124. Zhang Y, Hu Y, Lin J, Fan Y, Li Y, Lv Y and Liu X, ACS Appl. Mater. Interfaces, 2016, 8, 25454–25460. [PubMed: 27617695]

125. Han L, Liu SG, Dong JX, Liang JY, Li LJ, Li NB and Luo HQ, J. Mater. Chem. C, 2017, 5, 10785–10793.
126. Nie H, Li M, Li Q, Liang S, Tan Y, Sheng L, Shi W and Zhang SX-A, Chem. Mater, 2014, 26, 3104–3112.
127. Yuan K, Zhang X, Qin R, Ji X, Cheng Y, Li L, Yang X, Lu Z and Liu H, J. Mater. Chem. C, 2018, 6, 12631–12637.
128. Liu C, Wang R, Wang B, Deng Z, Jin Y, Kang Y and Chen J, Microcim. Acta, 2018, 185, 539–546.
129. Yuan F, Wang Z, Li X, Li Y, Tan Z. a., Fan L and Yang S, Adv. Mater, 2017, 29, 1604436–1604441.
130. Liu Z, Zou H, Wang N, Yang T, Peng Z, Wang J, Li N and Huang C, Sci. China Chem, 2018, 61, 490–496.
131. Gharat PM, Chethodil JM, Srivastava AP, Praseetha P, Pal H and Choudhury SD, Photoch. Photobio. Sci, 2019, in press.
132. Shen Z, Zhang C, Yu X, Li J, Wang Z, Zhang Z and Liu B, J. Mater. Chem. C, 2018, 6, 9636–9641.
133. Xu Q, Zhou Q, Hua Z, Xue Q, Zhang C, Wang X, Pan D and Xiao M, ACS Nano, 2013, 7, 10654–10661. [PubMed: 24251867]
134. Shamsipur M, Barati A, Taherpour AA and Jamshidi M, J. Phys. Chem. Letters, 2018, 9, 4189–4198.
135. Tang L, Ji R, Cao X, Lin J, Jiang H, Li X, Teng KS, Luk CM, Zeng S, Hao J and Lau SP, ACS Nano, 2012, 6, 5102–5110. [PubMed: 22559247]
136. Ren J, Weber F, Weigert F, Wang Y, Choudhury S, Xiao J, Lauermann I, Resch-Genger U, Bande A and Petit T, Nanoscale, 2019, 11, 2056–2064. [PubMed: 30644938]
137. Xiao L and Sun H, Nanoscale Horizons, 2018, 3, 565–597.
138. Liyanage PY, Graham RM, Pandey RR, Chusuei CC, Mintz KJ, Zhou Y, Harper JK, Wu W, Wikramanayake AH, Vanni S and Leblanc RM, Bioconj. Chem, 2019, 30, 111–123.
139. Zhou Y, Peng Z, Seven ES and Leblanc RM, J. Control. Release, 2018, 270, 290–303. [PubMed: 29269142]
140. Strauss V, Margraf JT, Dolle C, Butz B, Nacken TJ, Walter J, Bauer W, Peukert W, Spiecker E, Clark T and Guldi DM, J. Am. Chem. Soc, 2014, 136, 17308–17316. [PubMed: 25372278]
141. Wang S, Cole IS, Zhao D and Li Q, Nanoscale, 2016, 8, 7449–7458. [PubMed: 26731007]
142. Bourlinos AB, Stassinopoulos A, Anglos D, Zboril R, Karakassides M and Giannelis EP, Small, 2008, 4, 455–458. [PubMed: 18350555]
143. Ortega-Liebana MC, Chung NX, Limpens R, Gomez L, Hueso JL, Santamaria J and Gregorkiewicz T, Carbon, 2017, 117, 437–446.
144. Hola K, Bourlinos AB, Kozak O, Berka K, Siskova KM, Havrdova M, Tucek J, Safarova K, Otyepka M, Giannelis EP and Zboril R, Carbon, 2014, 70, 279–286.
145. Sciortino A, Marino E, Dam BV, Schall P, Cannas M and Messina F, J. Phys. Chem. Letters, 2016, 7, 3419–3423.
146. Zhang W, Yu SF, Fei L, Jin L, Pan S and Lin P, Carbon, 2015, 85, 344–350.
147. Hill SA, Benito-Alifonso D, Morgan DJ, Davis SA, Berry M and Galan MC, Nanoscale, 2016, 8, 18630–18634. [PubMed: 27801469]
148. Martindale BCM, Hutton GAM, Caputo CA, Prantl S, Godin R, Durrant JR and Reisner E, Angew. Chem. Int. Ed, 2017, 56, 6459–6463.
149. Cayuela A, Soriano ML, Carrillo-Carrión C and Valcárcel M, Chem. Commun, 2016, 52, 1311–1326.
150. Moon BJ, Oh Y, Shin DH, Kim SJ, Lee SH, Kim T-W, Park M and Bae S, Chem. Mater, 2016, 28, 1481–1488.
151. Sun Y-P, Zhou B, Lin Y, Wang W, Fernando KAS, Pathak P, Meziani MJ, Harruff BA, Wang X, Wang H, Luo PG, Yang H, Kose ME, Chen B, Veca LM and Xie S-Y, J. Am. Chem. Soc, 2006, 128, 7756–7757. [PubMed: 16771487]

152. Li H, He X, Kang Z, Huang H, Liu Y, Liu J, Lian S, Tsang CHA, Yang X and Lee S-T, Angew. Chem. Int. Ed, 2010, 49, 4430–4434.
153. Nguyen V, Yan L, Si J and Hou X, Opt. Mater. Express, 2016, 6, 312–320.
154. Tetsuka H, Asahi R, Nagoya A, Okamoto K, Tajima I, Ohta R and Okamoto A, Adv. Mater, 2012, 24, 5333–5338. [PubMed: 22833282]
155. Philippidis A, Spyros A, Anglos D, Bourlinos AB, Zbořil R and Giannelis EP,J. Nanopart. Res, 2013, 15, 1777–1785.
156. Bourlinos AB, Stassinopoulos A, Anglos D, Zboril R, Georgakilas V and Giannelis EP, Chem. Mater, 2008, 20, 4539–4541.
157. Weijian L, Chun L, Xiaobo S, Wei P, Guifeng Y and Jinping W, Nanotechnology, 2017, 28, 485705. [PubMed: 28961145]
158. Mintz KJ, Guerrero B, and Leblanc RM, J. Phys. Chem. C, 2018, 122, 29507–29515.
159. Peng Z, Miyanji EH, Zhou Y, Pardo J, Hettiarachchi SD, Li S, Blackwelder PL, Skromne I and Leblanc RM, Nanoscale, 2017, 9, 17533–17543. [PubMed: 29110000]
160. Krysmann MJ, Kelarakis A, Dallas P and Giannelis EP, J. Am. Chem. Soc, 2012, 134, 747–750. [PubMed: 22201260]
161. Roy P, Chen P-C, Periasamy AP, Chen Y-N and Chang H-T, Mater. Today, 2015, 18, 447–458.
162. Jin SH, Kim DH, Jun GH, Hong SH and Jeon S, ACS Nano, 2013, 7, 1239–1245. [PubMed: 23272894]
163. Yu J, Liu C, Yuan K, Lu Z, Cheng Y, Li L, Zhang X, Jin P, Meng F and Liu H, Nanomaterials, 2018, 8, 233–244.
164. Zhou Y, Mintz K, Oztan C, Hettiarachchi S, Peng Z, Seven E, Liyanage P, De La Torre S, Celik E and Leblanc R, Polymers, 2018, 10, 921–932.

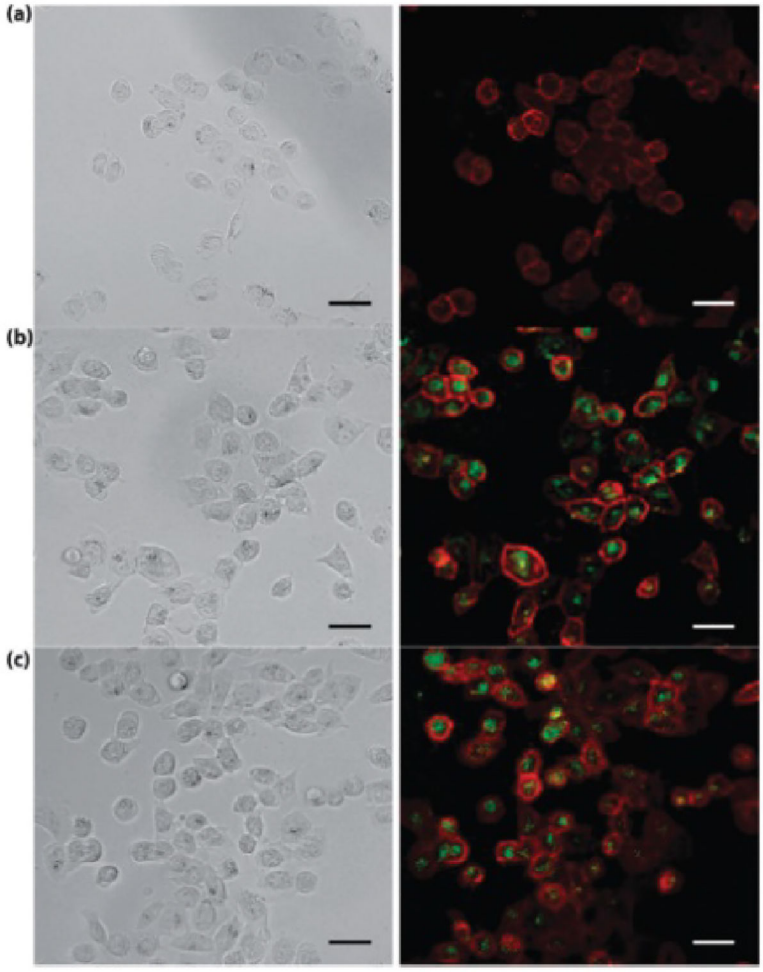

Figure 1.
Bright field and fluorescence images of: (A) H1299 cells. (B) H1299 cells incubated with CDs. (C) H1299 cells incubated with nanocomplexes of CDs and hyaluronic acid. Scale bar is 20 μm. Reproduced from Ref. 74 with permissions from The Royal Society of Chemistry.

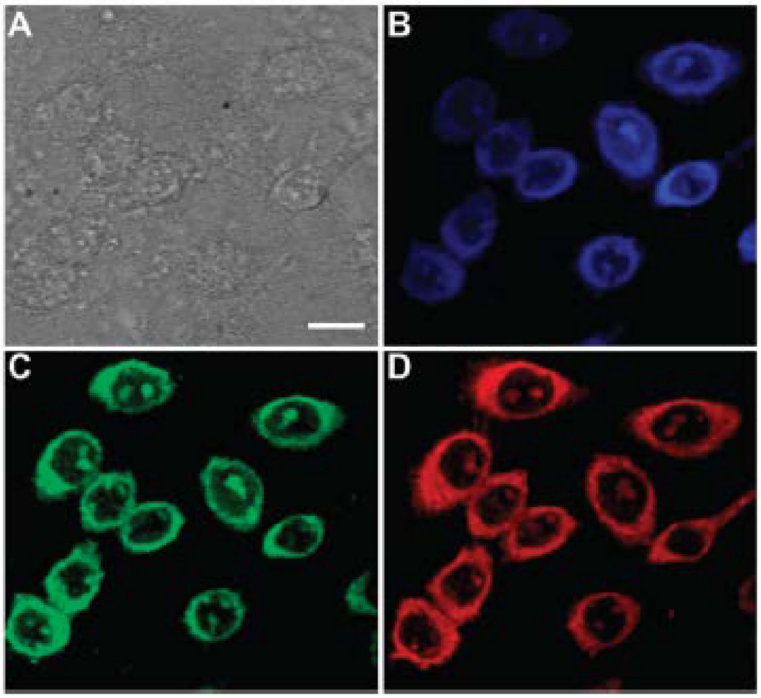

Figure 2.

CHO cells imaged by CDs. (A) Bright field image. (B) Confocal image excited at 405 nm. (C) Confocal image excited at 488 nm. (D) Confocal image recorded at 561 nm. Scale bar is 10 μm. Ref. 77- Published by The Royal Society of Chemistry.

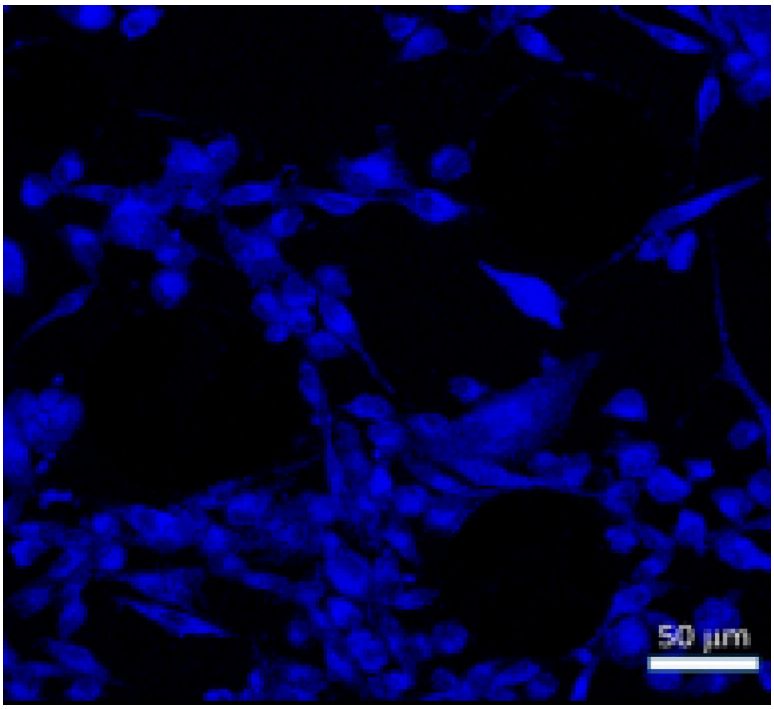

Figure 3.
Confocal image of CDs labeling the U87 cells. Adapted with permission from Ref. 84. Copyright 2014 American Chemical Society.

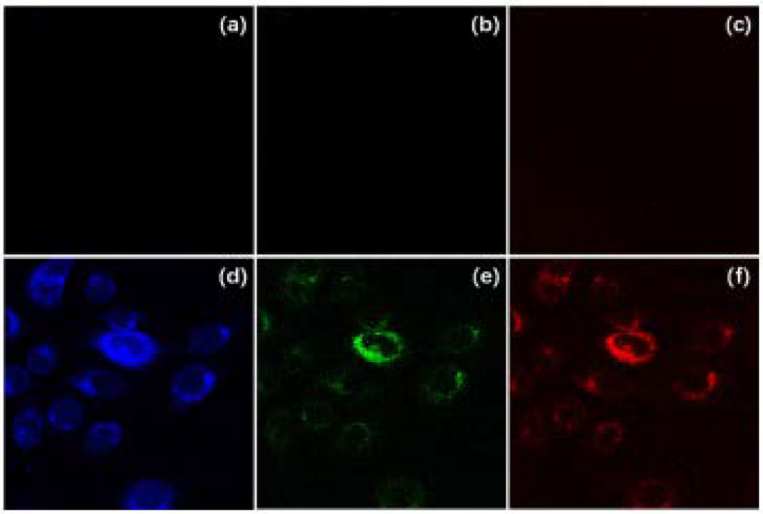

Figure 4.

HaCaT cell confocal images without (a-c) and with (d-f) 500 μg/mL CDs. Images a and d are excited at 405 nm, b and e are excited at 488 nm, c and f are excited at 543 nm. Figure adapted from Ref. 86 with permission Korean Carbon Society.

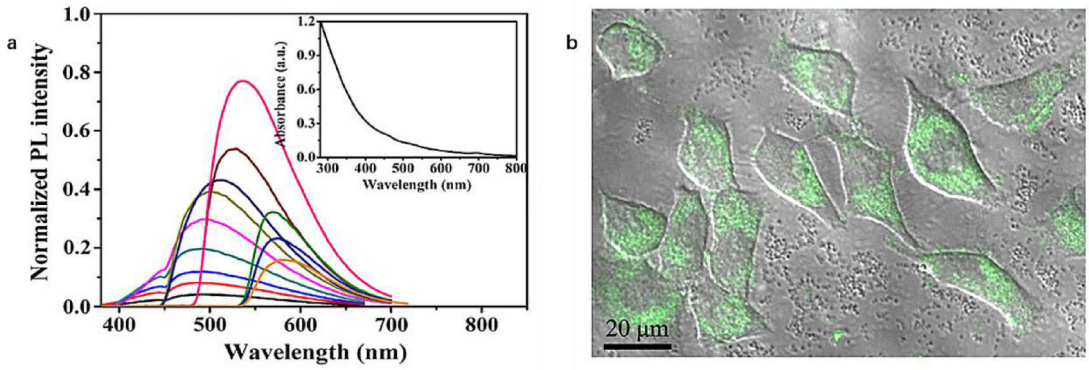

Figure 5.

(a)Normalized PL emission spectrum with excitation wavelength increasing from 310 nm in 20 nm increment (inset: UV/vis absorption spectrum of CDs obtained); (b) Confocal microscopy image of Hela cell incubated with CDs (λex =488 nm). Figure adapted from Ref. 82 with permissions from Elsevier.

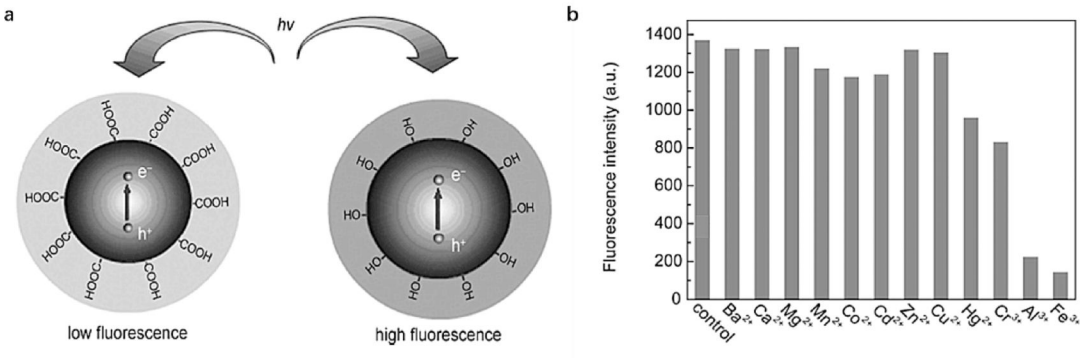

Figure 6.

(a) The schematic illustration of PL emission of hydroxyls-coated CDs better than the regular carboxyls-coated CDs (e^-: electrons, h^+: holes); (b) The PL quenching effect of CDs by different metal ions (λex =310 nm). Figure adapted from Ref. 20 with permissions from Springer.

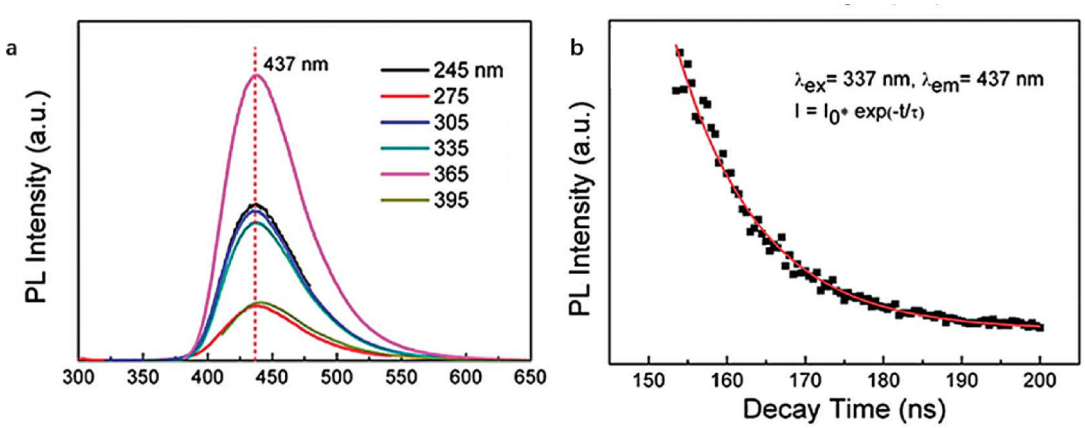

Figure 7.

PL emission spectrum of CDs excited from 245 to 395 nm (a); PL decay lifetime profile of the CDs (b). Figure adapted from Ref. 58 with permission The Royal Society of Chemistry.

a Photoluminescence lifetime and quantum yield (QY) of carbon colloids fabricated at 130, 160, 200 and 240°C. The highest QY was achieved at 160°C

Sample	τ_1 (ns)	τ_2 (ns)	τ_{ave} (ns)	QY %
130°C	**6.78**	**--**	**6.78**	**35.4**
160°C	**7.13**	**--**	**7.13**	**44.7**
200°C	**2.81**	**10.41**	**6.12**	**28.1**
240°C	**3.51**	**9.85**	**5.21**	**20.8**

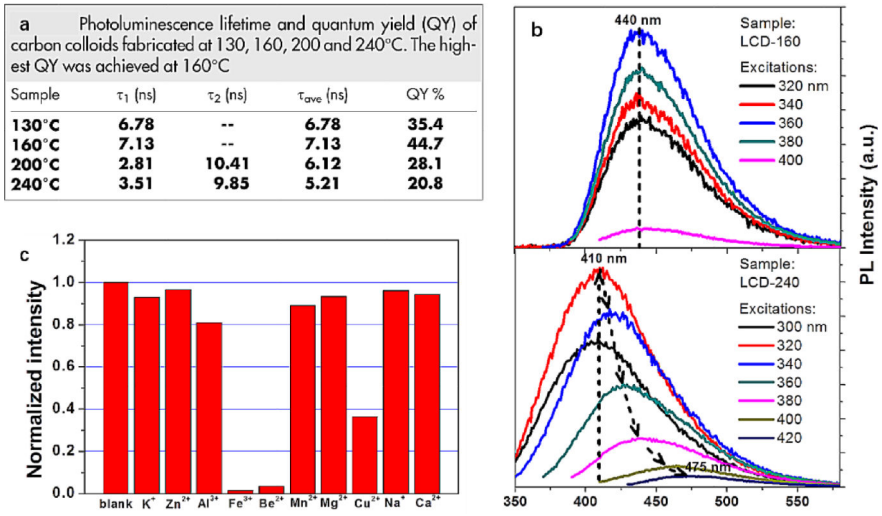

Figure 8.

PL decay lifetime and quantum yield of CDs made at 130, 160, 200 and 240 °C (a); The PL emission spectra of CDs made at 160 and 240 °C (b); The quenching effect of different ions on the CDs. Figure adapted from Ref. 106 with permissions from Nature Research.

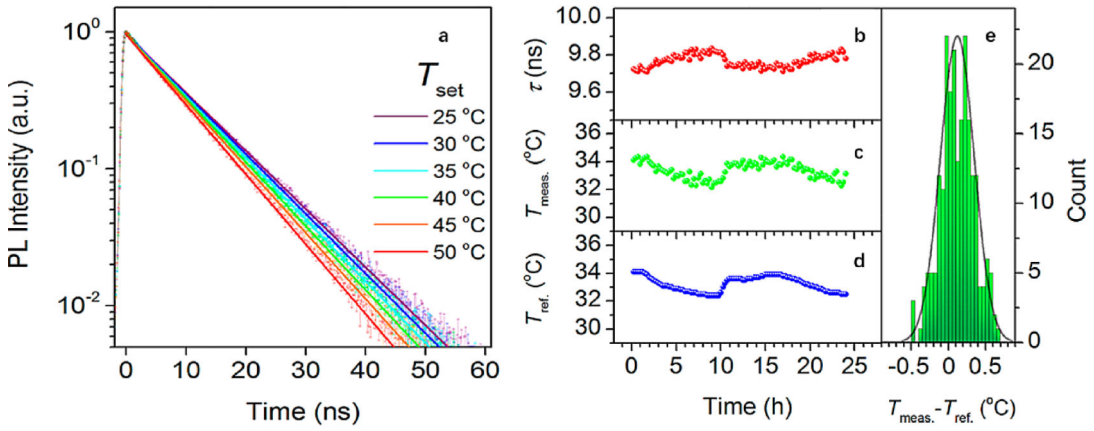

Figure 9.

(a) PL emission decays of HeLa cells cultured in CDs aqueous solution with a concentration of 500 μg/mL at different temperatures; (b) PL decay lifetimes extracted from the PL transients recorded every 15 min for 24 h of HeLa cells cultured in CDs aqueous solution (500 μg/mL); (c) Temperatures obtained using the calibration curve based on a calibration curve described by an equation: $T = 330.59–94.99\tau+11.87\tau^2-0.54\tau^3$, $R_{adj}^2=0.998$, T, temperature; τ, lifetime; (d) Temperatures measured by a reference thermometer; (e) Histogram revealing the deviation between (c) and (d), the solid line is the distribution curve. Figure adapted from Ref. 23 with permissions from the American Chemical Society.

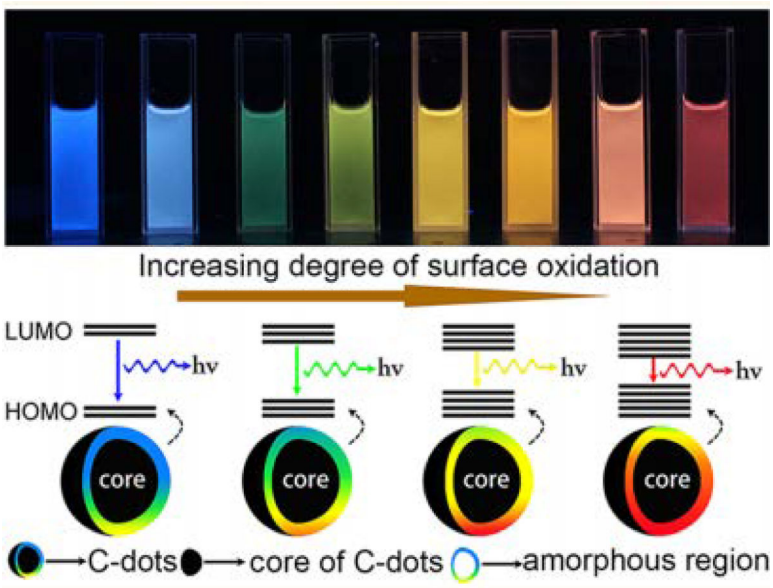

Figure 10:
Image of different CDs fractions under UV light and the modeling of their bandgap based on surface oxidation. Figure adapted from Ref. 122 with permissions from the American Chemical Society.

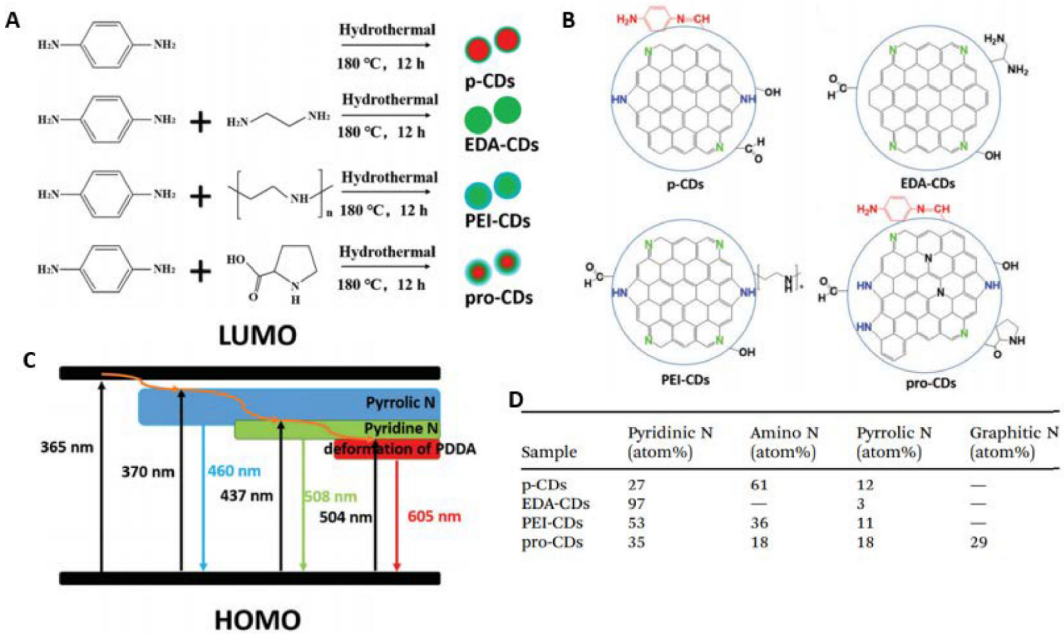

Sample	Pyridinic N (atom%)	Amino N (atom%)	Pyrrolic N (atom%)	Graphitic N (atom%)
p-CDs	27	61	12	—
EDA-CDs	97	—	3	—
PEI-CDs	53	36	11	—
pro-CDs	35	18	18	29

Figure 11:

(A) Summary of preparation of CDs. (B) Proposed representative structure for each CDs. (C) Proposed energy level diagram for surface states of CDs. (D) Nitrogen percentages in CDs samples. Figures adapted from Ref. 127 with permissions from The Royal Society of Chemistry.

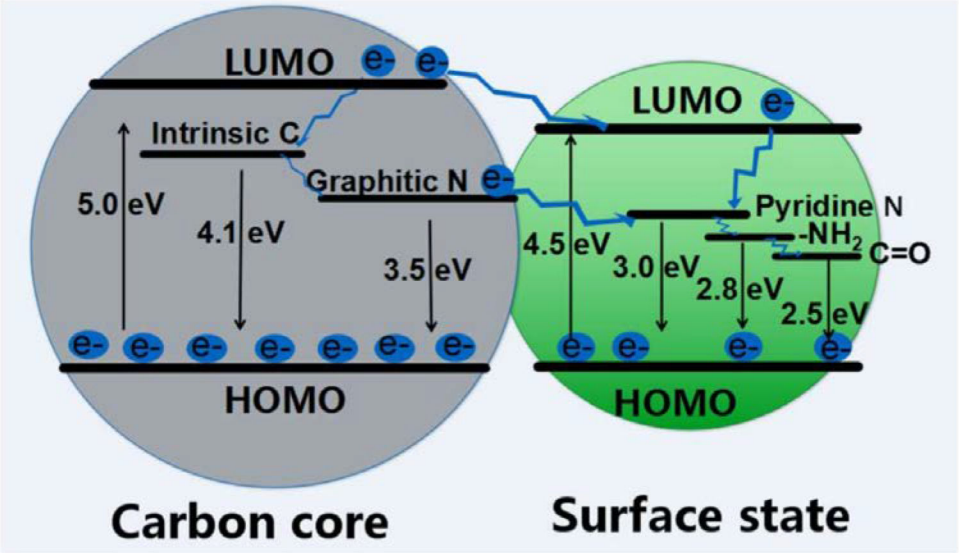

Figure 12:
A scheme of energy band structure and possible PL process for CDs. Figure adapted from Ref. 163 with permission from MDPI.

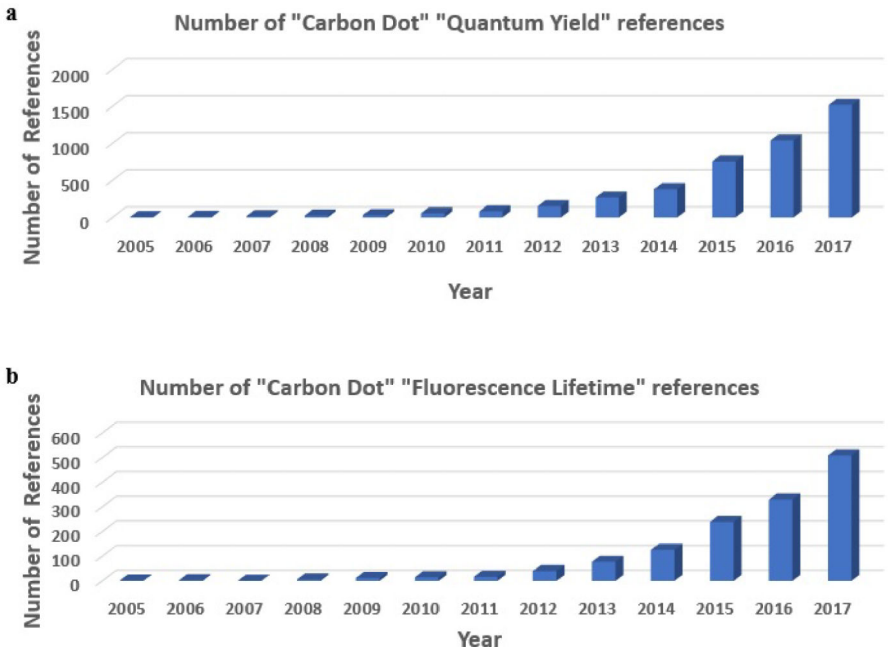

Scheme 1.

(a) Histogram showing number of references related to CDs and QY per year. (b) Histogram showing number of references related to CDs and fluorescence lifetime per year (Note: while not the correct technical term, fluorescence lifetime is the term used most often in the literature to describe the PL decay lifetime of CDs).